Evolutionary dynamics of the arthropod moulting machinery

Giulia Campli[1,2], Sagane Joye[1,2], Olga Volovych[3], Asya Novikov[3], Ariel D. Chipman[3], Marc Robinson-Rechavi[1,2], Robert M. Waterhouse[2]

[1] Department of Ecology and Evolution, University of Lausanne, 1015, Lausanne, Switzerland.

[2] SIB Swiss Institute of Bioinformatics, 1015, Lausanne, Switzerland.

[3] The Department of Ecology, Evolution and Behaviour, The Hebrew University of Jerusalem, Edmond J. Safra Campus, Givat Ram, Jerusalem, 9190401, Israel.

Abstract

Exoskeletons define arthropods, providing support for segmented bodies and appendages while protecting against environmental stress and predation. Although ubiquitous, this evolutionarily variable feature has enabled arthropods to occupy diverse lifestyles and ecological niches, contributing to their unrivalled diversity. Because the chitinous cuticle is rigid, exoskeletons must be periodically shed and replaced as animals grow. Arthropods therefore develop through discrete moults, with conserved phases that progress from pre-moult preparation to ecdysis and post-moult maturation. These are tightly regulated developmental transitions controlled by a molecular toolkit comprising neuropeptides, hormone-synthesising enzymes, receptors, and the early, fate, and late gene sets that activate and execute the moulting process. Although genetic studies in model species have identified many components, major knowledge gaps remain, especially in non-insect arthropods. Advances in genome sequencing now enable comparative genomic analyses across diverse, previously understudied arthropod lineages to begin to address these gaps. We present a comprehensive comparative genomic survey of arthropods, sampling all four major subphyla: Chelicerata, Myriapoda, Crustacea, and Hexapoda. Orthology inference and copy-number analyses contrast stable and dynamic components of the moulting machinery across the phylum. Ancestral state reconstructions and phylogenetic reconciliations reveal gene duplication and loss dynamics and the evolutionary histories of key moulting gene families. The inclusion of newly generated myriapod genomes addresses a major taxonomic gap and enables inferences of gene repertoire changes in the Mandibulata ancestor. The broad taxonomic representation enables a phylum-wide assessment to systematically evaluate, refine, and revise current understanding of the evolutionary dynamics of the entire moulting genetic toolkit.

Introduction

Development via periodic moulting represents a hallmark of all extant arthropod lineages and their extinct ancestors, where their exoskeletons provide both physical support and protection but need to be replaced to allow for normal growth and maturation. Arthropod life histories are therefore punctuated by ecdysis events, when internal pressure opens fractures along sutural lines in the rigid chitin, allowing the individual to escape from the former exoskeleton and replace it with a new one. Synthesis of the new, larger exoskeleton starts well before this ecdysis event, which is in fact part of a broader process that also includes a preparatory phase before the exit from the exuviae, and a terminal phase encompassing the maturation of the newly formed sheath. These phases may vary greatly across species in time span, and substantial heterogeneity is observed in the number of moults occurring during the entire life cycle. For example, a fruit fly undergoes only three moults over the course of a few days, while the horseshoe crab *L. polyphemus* normally moults yearly throughout decades (Tetlie et al. 2008). Large variations are also found in the length of the intermoult, that is the intervening period between two moults, where the arthropod feeds and grows until reaching a size where the exoskeleton constrains growth (Nijhout et al. 2014). Remarkably, moulting allows growth not only by an increase in body dimensions but also by the postembryonic addition of new segments (Fusco & Minelli 2021; Chipman 2025). This process of anamorphosis characterises the development of several lineages, both extinct, such as Trilobita and other arthropod stem-groups, and extant, such as the early branching pycnogonid chelicerates, all diplopod myriapods and many centipedes, and several non-hexapod crustaceans (Fusco & Minelli 2021). In contrast, epimorphic development proceeds with no changes in the number of segments after hatching. Moulting is therefore both a ubiquitous yet highly variable process, which has enabled arthropods to adopt a wide variety of lifestyles and to exploit different ecological niches across all environments, for example in holometabolous insects it mediates the characteristic metamorphic transition to adulthood via a pupal stage.

Moulting events are carefully orchestrated transitionary processes in normal growth and development controlled by a toolkit of molecular components including neuropeptides, hormone-synthesising enzymes, and receptors, as well as the so-called early, late, and fate genes (Campli et al. 2024). Studies in insects and other arthropods have clearly highlighted that the ecdysteroid and sesquiterpenoid hormone receptors are the main moulting signal transducers, activated by hormones synthesised by enzymatic pathways that are triggered by moult-inducing environmental or endogenous stimuli (Qu et al. 2015). Such hormonal

pathways lead to the activation of regulatory networks of transcription factors that control the expression of sets of genes coding for structural components of the exoskeleton. Finally, declining hormonal titres initiate irreversible neuroresponses, culminating in ecdysis and post-ecdysis exoskeleton maturation. The identification and characterisation of these many molecular components that make up the moulting machinery has advanced through research leveraging well-established genetic techniques for experimental manipulations of a few tractable model species. This means that across the accumulated knowledge from experimental laboratory studies there remain substantial gaps in our understanding of the molecular mechanisms underlying the moulting process (Campli et al. 2024). Nevertheless, new opportunities to begin to address these gaps are growing rapidly as advances in sequencing technologies are enabling the generation of large amounts of genomics data. These accumulating resources facilitate the comparative exploration of relatively understudied arthropod lineages (Feron & Waterhouse 2022a, 2022b), to investigate putative moulting toolkit components by analysing the genomes of an increasing number of species.

Here we present the results from conducting an extensive comparative genomic survey of a large set of arthropod species including representatives of all four major arthropod subphyla: Chelicerata, Myriapoda, Crustacea, Hexapoda, where hexapods and the paraphyletic crustaceans together form the monophyletic Pancrustacea. The survey results enable a phylum-wide assessment of the stable and dynamic components of the moulting machinery through comprehensive orthology delineation and copy-number profiling of genes belonging to the main functional modules involved in moulting. Employing ancestral state reconstructions and phylogenetic reconciliations we investigate the evolutionary histories of moulting gene families across the arthropod phylogeny. Furthermore, *de novo* genome sequencing of myriapods contributes to the knowledge of this heretofore poorly represented subphylum, as well as allowing for the pinpointing of gene repertoire changes to the Mandibulata ancestor. The results extend, in a systematic manner, the taxonomic breadth of interrogated lineages and serve to confirm, challenge, and revise reports from the literature on the presence and putative functionality of moulting genetic toolkit components across Arthropoda.

Results

Broad taxonomic representation enables a phylum-wide assessment of the moulting machinery

Assessing and collating available and newly generated annotated arthropod genomes resulted in a dataset of 145 species spanning the four major lineages of Chelicerata, Myriapoda, Crustacea, and Hexapoda, comprising 35 orders, 57% of which are represented by multiple species (Figure 1). Sampling from publicly available genomic resources aimed to build a representative dataset that included arthropod species from different orders, and selecting the best quality assemblies and annotations from over-represented clades (mainly insects) aimed to balance taxonomic representation across the phylum. To include Myriapoda representatives in the dataset, genome sequencing, assembly, and annotation were performed for three species, *Scolopendra cingulata* (Mediterranean banded centipede) and *Scutigera coleoptrata* (house centipede) from the class Chilopoda, and *Archispirostreptus syriacus* (black millipede) from the class Diplopoda. To investigate the evolutionary histories of genes implicated in moulting processes, this phylum-wide dataset was used to define the species and order-level phylogenies (Figure 1A) and to delineate orthologous groups (OGs) at the last common ancestor (LCA) of Arthropoda (Figure 1B). Species tree estimation from single-copy orthologues resulted in a phylogeny congruent with previous large-scale phylogenomics findings (Misof et al. 2014; Schwentner et al. 2018; Howard et al. 2020). Graph-based orthology delineation resulted in the clustering of 80% of all annotated protein-coding genes into 74’214 OGs, each representing all genes descended from a single gene in the LCA. Together, the time-calibrated species phylogeny and orthology data (Supplementary Figure 1) provide the basis for reconstructing gene family evolutionary histories including duplication and loss events across the phylum over the last ~600 million years of arthropod evolution.

Querying the orthology dataset with curated lists of moulting machinery genes, *i.e.* components of the functional modules of moulting processes known from emerging and model systems, resulted in the identification of 63 OGs containing a total of 19’015 genes. The lists were based on extensive reviews of the accumulated knowledge of the genetic toolkit governing arthropod moulting (Campli et al. 2024), comprising 76 gene families with evidence of involvement in various moulting processes. Based on the roles they play, these gene families can be grouped into six functional modules: the ecdysteroid and sesquiterpenoid pathways for hormone synthesis and signalling, the early gene and fate

gene sets for activation of the moulting-induced programme, the toolkit of receptors of neuropeptides switching on the moulting process, and downstream late gene effectors for exoskeleton renewal. Contrasting the evolutionary histories of these functional modules in terms of the phyletic ages (Figure 1C) and levels of protein sequence divergence (Figure 1D) of their constituent OGs revealed the ancient origin of almost all families, showing both high and low levels of sequence divergence.

Gene family phyletic ages are defined as the LCA of all the species included in the family, simplified to stratifications of Arthropoda, Mandibulata, the four subphyla, and younger than subphylum level. The 145-species dataset allows for the designation of OGs spanning the Chelicerata-Mandibulata root to be at least as old as the arthropod ancestor, *i.e.* OGs assigned a phyletic age of Arthropoda LCA may be older. All but two of the moulting machinery gene families were traceable to the arthropod ancestor, reflecting the ancient origins of genes involved in moulting processes (Figure 1C). This is in contrast to the background of all other gene families, for which only 26% of OGs were traceable to the arthropod LCA with more than half emerging after the divergence of the four subphyla (Figure 1C). Emergences of new gene families, *i.e.* genes for which orthology can be traced to an internal node of the phylogeny but not to the arthropod root, therefore appear to contribute little to the evolution of the moulting machinery. However, functional studies in the many less well studied arthropod lineages may yet reveal novel innovations, whose origins can then be traced using comparative analyses across the phylum.

Gene family evolutionary rates quantify sequence-level dynamics in terms of the levels of protein sequence divergence amongst their member genes. Compared to the background of all other OGs, the moulting machinery gene families show overall significantly lower evolutionary rates, consistent with expected constraints associated with such an ancient and developmentally critical process (Figure 1D). While each moulting functional module shows some variation in evolutionary rates, the overall most divergent ecdysteroid pathway module is significantly higher than the early, late, and fate gene modules (Figure 1D). The sesquiterpenoid pathway module shows the same trend, but these differences are not statistically significant. Therefore, while genes implicated in moulting processes are generally more conservatively evolving in terms of protein sequence divergence, members of the ecdysteroid and sesquiterpenoid modules including hormone-synthesising enzymes and receptors show elevated evolutionary rates compared to the other modules.

Gene copy-number profiling reveals stable and dynamic components of the moulting machinery

To contrast stably evolving and dynamic gene families, phylogenetic profiling of gene copy numbers resulted in quantified counts of identified orthologues across the 145-species dataset, partitioned by the 35 orders and six functional modules (Figure 2). This characterisation shows that gains and losses of genes involved in moulting are evident across all modules and nearly all orders. While the sesquiterpenoid pathway and early genes modules exhibit mainly single-copy orthologues, the ecdysteroid pathway and late genes show elevated proportions of duplications, and the neurostimuli module exhibits the lowest proportion of single-copy orthologues. Detection of single- or multiple-copy orthologues provides evidence of the maintenance of each gene family across taxa. Failure to detect orthologues may represent true gene losses, however, follow-up investigations are required to support the loss hypothesis. Therefore, interpreting these profiling results focuses on cases where absences from multiple species lend support to likely lineage-wide loss events. The order by module profiling analysis presented in Figure 2 reveals broad trends across the sampled arthropod lineages that are nevertheless characterised by striking variability of the member gene families within each module (Supplementary Figures 2-7).

Of the two pathways for hormone synthesis and signalling, the ecdysteroid pathway exhibits an overall lower proportion of gene families with single-copy orthologues across the phylum than the sesquiterpenoid pathway (Figure 2). This trend is driven mainly by extensive duplications of genes encoding ecdysteroid biosynthetic cytochrome enzymes as well as transporters for ecdysteroid trafficking, with other pathway members showing more conservative evolutionary histories (Supplementary Figure 2). The cytochrome P450 monooxygenase (CYP) genes include *spook* (*spo*, cyp307a1), *spookier* (*spok*, *cyp307a2*), *phantom* (*phm*, *cyp306a1*), *disembodied* (*dib*, *cyp302a1*), *shadow* (*sad*, *cyp315a1*), *shade* (*shd*, *cyp314a1*), and *cyp18a1* (Pan et al. 2021). With two gene copies in most insects and some crustaceans the profiling results agree with previous observations indicating that *spook* was present in the arthropod ancestor while its paralogue emerged in the pancrustacean ancestor but not the Mandibulata ancestor (Schumann et al. 2018). While *disembodied*, *shadow*, and *shade* are generally found as single-copy orthologues, the family containing *phantom* and *cyp18a1* is highly expanded –most orders have 10 or more genes– and includes the cyp15 epoxidase cytochromes. The complexities of lineage-specific expansions of CYP clans mean that homology-based inferences may be unreliable, and

hypotheses on gene function require biochemical experiments to understand which of these enzymes in each species is responsible for each biosynthetic reaction (Campli et al. 2024).

The families of transporters for ecdysteroid trafficking exhibiting expansions include the ATP-binding cassette (ABC) transporter expressed in trachea (Atet) and the Ecdysone Importer (Ecl). Responsible for loading ecdysone into secretory vesicles for subsequent release into the circulatory system (Pan et al. 2021), Atet belongs to subfamily G of the ABC transporter superfamily, which has substantially expanded in insects, and in contrast, has lower gene counts in species of the order Mesostigmata (Denecke et al. 2021). Across the 35-order dataset, large family sizes predominate across the insect orders, in several lineages of Acari, and in two of the three myriapod species (Supplementary Figure 2). The family that includes EcI shows generally modest expansions compared to Atet, with 3-9 genes across most orders, and with the largest counts found in non-Hexapod orders (Supplementary Figure 2). EcI is also known as Organic anion transporting polypeptide 74D (Oatp74D), and mediates ecdysone uptake by target cells in peripheral tissues (Okamoto & Yamanaka 2021; Samantsidis et al. 2022; Wellmeyer et al. 2023). As with the cytochromes, identifying functionally equivalent genes involved in ecdysteroid trafficking from amongst the Atet and EcI family expansions would require experimental investigations.

Amongst other ecdysteroid pathway gene families, we report here, to the best of our knowledge, the first identification of *shroud* (*sro*, also named *non-molting-glossy*) beyond model insects. *Shroud* encodes a short-chain dehydrogenase/reductase that functions in the 'Black Box' of the ecdysteroid biosynthesis pathway (Niwa et al. 2010), found across all arthropod orders in the orthology dataset except in Isopoda (Supplementary Figure 2). The sterol regulatory element binding protein (SREBP) is known in insects as an important lipid sensor, while in the shrimp *Litopenaeus vannamei* it has been found to be involved in regulating ecdysteroidogenesis (Xiaojun Zhang et al. 2019; Jing & Behmer 2020; Zheng et al. 2022). The results extend the breadth of previous observations in insects and a few decapod species to chelicerates and thus to the arthropod ancestor (Supplementary Figure 2). Additionally, the results indicate that a single gene coding for the membrane steroid binding protein (MSBP) was present in Arthropoda ancestor (Supplementary Figure 2). In *D. melanogaster* cell lines ecdysone sequestration by MSBP suppresses ecdysone signalling (Fujii-Taira et al. 2009). Finally, the Ecdysone Receptor (EcR) has likely been duplicated in daphnids from the order Diplostraca, and its partner Ultraspiracle (Usp, also known as Retinoid X Receptor, RXR) is found in two copies in roughly 75% of Araneae, Mesostigmata, Ixodida, and Sarcoptiformes species (Supplementary Figure 2).

The sesquiterpenoid pathway, which produces hormones such as juvenile hormone (JH) and methyl farnesoate (MF), exhibits much higher proportions of components that are recovered as single-copy orthologues in most orders compared to the ecdysteroid pathway (Figure 2). The exceptions to this are the JH epoxide hydrolase (JHEH) and JH acid methyl-transferase (JHAMT) families, with multi-copy orthologues in a majority of orders (Supplementary Figure 3). In insects, JHEH and JHAMT share JH acid as a substrate, but they mediate reactions in opposite directions; while JHAMT can catalyse the formation of JH to stimulate JH-induced biological responses, JHEH activity leads to JH diol acid and irreversible inactivation of JH (Qu et al. 2015; Smykal & Dolezel 2023; Campli et al. 2024). Both show expansions mainly in Hexapoda, with more than 50% of the species in multi-species orders having at least two copies. A similar pattern of duplications is seen in Chelicerata (Supplementary Figure 3). In Myriapoda and Crustacea they are mostly found as single-copy orthologues, except for some lineages within Malacostraca, where JHAMT might have been lost and JHEH duplicated, although a more extensive taxonomic representation is required to confirm this pattern.

JH synthesis is considered to be an insect innovation, so the experimental study of sesquiterpenoid pathway components is heavily biased towards holometabolan model systems, with genomic analyses being limited to modest datasets comprising only a few non-insect arthropod representatives (Li et al. 2007; Sin et al. 2015; Qu et al. 2015; Wang et al. 2022; Campli et al. 2024). The profiling results support the presence of all key components of the JH pathway in the arthropod ancestor (Supplementary Figure 3). This is interesting given that most of their characterised roles are based on the study of JH in insects, with little exploration of how they might interact with MF or farnesoic acid (FA) in other arthropods. The presence of these components in the arthropod ancestor suggests they were ancestrally involved in sesquiterpenoid processing, an idea supported by the known ability of methoprene-tolerant (Met) to bind MF (Miyakawa et al. 2013). In insects, JH-mediated signalling FK506-binding protein 39kD (FKBP39) and calponin homology domain protein 64 (Chd64) bind to JH-responsive DNA elements; JH binding protein (JHBP) and JH esterase binding protein (JHEBP) are known for their roles in JH sequestration; Met and its partner Taiman (tai) are known as JH receptors. All of these JH-associated proteins could have ancestrally targeted other hormonal forms or intermediates. While not as widespread or large as for JHEH and JHAMT, duplications are also observed for Met. One duplication has been documented in the fruit fly and tsetse fly, with the paralogue *germ cell-expressed* (*gce*) exhibiting partially overlapping but not fully redundant functions. Two copies have also been found in the silkmoth *Bombyx mori* (Daimon et al. 2015; Jindra et al. 2015). The profiling results extend identified putative *met* paralogues also in Blattodea, Ephemeroptera,

Diplostraca, Decapoda, Podocopida, Trombidiformes, and Araneae (Supplementary Figure 3), suggesting that multiple copies for fine regulation of immature phenotype gating might also be found beyond Holometabola.

The set of early genes, transcription factors activated just after hormone stimulation, is the module with the most single-copy orthologues across the orders (Figure 2). A notable exception is the Xiphosura horseshoe crab, which has multiple copies for each gene family (Supplementary Figure 4). This is based on only a single species but is consistent with three rounds of whole genome duplications in the horseshoe crab lineage (Nong et al. 2021; Castellano et al. 2025). Interestingly, these genes have been maintained despite apparently strong constraints to avoid duplication across the rest of the phylum. In the orthology dataset the Ecdysone-inducible genes 75 (*E75*) and 78 (*E78*) are clustered in the same OG, however these were likely both present in the ecdysozoan ancestor (Schumann et al. 2018). In this otherwise well-maintained set of gene families a plausible loss could have occurred of the gene encoding Hormone Receptor 96 (HR96), a nuclear receptor that is inducible by 20E and binds cholesterol (Fisk & Thummel 1995; Jing & Behmer 2020). It was previously reported missing from the aphid *Acyrthosiphon pisum* (Bonneton & Laudet 2012), and here HR96 appears to be absent from more than half the Hemiptera species in the orthology dataset, as well as being undetectable in any of the mites of the order Mesostigmata (Supplementary Figure 4). Together with the potential losses of the neverland (nvd) enzyme for cholesterol processing and the Atet transporter, these results favour the hypothesis that novel pathways might have emerged in mites in relation to parasitic lifestyles and synchronisation to host metabolism (Cabrera et al. 2015; Aurori et al. 2021).

The small set of fate genes is characterised by a notable pattern of missing genes outside of hexapods (Figure 2). This is mainly due to the presumed emergence of the larval determinant transcription factor, chronologically inappropriate morphogenesis (*chinmo*), in the hexapod ancestor. Chinmo is essential for maintaining the larval stage in *Drosophila*, in opposition to two other fate genes, *broad* and *ecdysone-inducible gene 93* (*E93*) (Truman & Riddiford 2022). The other immaturity determinant, Kruppel homolog 1 (*Kr-h1*), appears to have been repeatedly lost in chelicerates, since no orthologues were detected in at least 50% of species from Araneae and Acari orders, and in any of Trombidiformes, while several other chelicerates do have identifiable orthologues (Supplementary Figure 5). Sarcoptiformes appears to have the most incomplete set, with 86% of the surveyed species also missing the adulthood specifier *E93*. In contrast, the broad gene family exhibits a complex history with many BTB/POZ (broad complex Tramtrack bric-a-brac/Pox virus and

zinc finger) transcription factors clustering together resulting in more than three copies throughout Arthropoda (Supplementary Figure 5).

The neurostimuli module exhibits the lowest proportion of single-copy orthologues, with multiple copies of the genes coding for neuropeptide receptors triggering moulting in all the four subphyla. Between 60% and 80% of pathway components are duplicated, often with multiple copies in well-represented orders (Figure 2). This is particularly striking for the eclosion hormone receptor (EHR) and Rickets (rk) gene families (Supplementary Figure 6), suggesting the presence of multiple copies in the Arthropoda ancestor. In insects, ecdysis triggering hormone receptor (ETHR) is known to have multiple isoforms that might have acquired different specialisations (Campli et al. 2024), thus isoform sequence evolution and lack of accuracy in isoform annotation in non-model species might inflate the number of putative paralogues (Supplementary Figure 6). Although the ecdysis neuromotor signal reception components are complete in other chelicerates, they are missing from more than 50% of Sarcoptiformes and Mesostigmata species (Supplementary Figure 6). Previous investigations reported conflicting results for these components, especially for the existence of the crustacean cardioactive peptide receptor (CCAP-R) signal (Campli et al. 2024).

The late genes exhibit elevated proportions of duplications, similar to the ecdysteroid pathway (Figure 2). The module comprises genes involved in exoskeleton assembly such as the enzymatic effectors necessary for synthesis, remodelling, spatial arrangement, and cross-linking the building blocks of chitin and cuticle proteins (CPs). The superfamily of CPs is not included in the profiling analysis due to its large and complex nature (Willis 2010) and its largely structural role in moulting processes. Across the multi-species orders in the dataset, from 31% (Hymenoptera) to 70% (Araneae) of the late effector genes were detected at least in double-copy (Figure 2). Amongst the chitinases, Cht2, Cht4, Cht8, and Cht9 cluster together in a large multi-copy group spanning all orders in contrast to the most conservative Cht7 that is almost universally single-copy (Supplementary Figure 7). A key effector step is cuticle hardening, achieved in insects mainly by cross-linking CPs with oxidised catechol derivatives, as in the pathway for melanin synthesis (Campli et al. 2024). This oxidation is mediated by the laccase enzyme straw (stw), paralogue of the multicopper oxidase1 (mco1), from a large superfamily of multicopper oxidases (Asano et al. 2019; Janusz et al. 2020). The profiling analyses suggest the absence of stw or mco1 orthologues in any chelicerate lineage (Supplementary Figure 7), although related multicopper oxidases may be present. No studies to-date have fully characterised the mechanisms for cuticle hardening in chelicerates, in fact discovery of melanin itself is relatively recent (Hsiung et al. 2015), and the absence of mco has been preliminarily explored only in four chelicerates

(Asano et al. 2019). Therefore, in lineages where post-ecdysis hardening of the exoskeleton is poorly understood, mechanisms based on under-explored cross-linking substrates such as resilin are of particular interest. Resilin is a matrix protein that cross polymerises by tyrosine-mediated bonds and thus gives elastic resistance to joints, tendons, or wings, in locusts, dragonflies, and flies. Surprisingly, it has been found at high concentration in a copepod 'tooth' specialised to break hard diatom shells (Michels et al. 2012; Lerch et al. 2020, 2022). The profiling results reveal more than three copies of resilin-like genes across different arthropod orders and at least ten copies in 67% of Araneae species and in some crustaceans, a few Podocopida, a copepod, and a barnacle (Supplementary Figure 7), indicating a putative role for diverse resilins in many arthropods.

Moulting toolkit insights from three new myriapod genomes

Mandibulata comprises a monophyletic clade including Pancrustacea and Myriapoda (Chipman 2024). Genomic sampling of Myriapoda remains extremely limited relative to the other subphyla, therefore, sampling additional myriapod species helps to build a better characterisation of this lineage, and to investigate changes occurring in the mandibulate ancestor. Genome assemblies were produced from Pacific Biosciences HiFi sequencing reads with estimated coverage of 40x to 47x resulting in genomes of 1.5 Gbp (600 contigs), 2.2 Gbp (344 contigs), and 1.5 Gbp (3'887 contigs) for *S. cingulata*, *S. coleoptrata*, and *A. syriacus*, respectively (see Materials and Methods). Genome annotation employed RNA sequencing data to predict gene models for each assembly, resulting in sets of 17'995, 18'157, and 11'437 protein-coding genes for *S. cingulata*, *S. coleoptrata*, and *A. syriacus*, respectively, with completeness scores of between 95% and 98%.

In-depth inspection of the annotated genomes of the centipedes, *S. cingulata* and *S. coleoptrata*, and the millipede, *A. syriacus*, revealed several potentially relevant lineage specific peculiarities in hormone synthesis and response, with an otherwise strong conservation of the rest of the arthropod moulting toolkit (Figure 3). In the three species, 41% of gene families were recovered as single-copy orthologues in both Chilopoda and Diplopoda, and 13% as duplicated with at least two copies in both classes. Duplication and loss events in myriapods generally reflect the observed arthropod-wide patterns. These include a propensity for duplications of the *phm* and *cyp15* cytochromes (Supplementary Figure 2), as well as frequent detection of multi-copy families for EcI (Supplementary Figure 2), Broad (Supplementary Figure 5), EHR (Supplementary Figure 6), chitinases and chitin deacetylases (Supplementary Figure 7). The analysis of the myriapod genomes indicated

that the duplication of spo-like *cyp307* genes does not extend beyond Pancrustacea (Supplementary Figure 2), and that *chinmo* was not present in the mandibulate ancestor (Supplementary Figure 5).

The absence of a JHAMT orthologue from the millepede *A. syriacus* (Figure 3) is congruent with the hypothesis that millipedes, unlike centipedes, use farnesoic acid (FA) as their main moulting hormone, since they are not able to further transform it into methyl farnesoate (So et al. 2022). It is worth noting that millipedes might also have alternative strategies for ecdysteroid stimulation, suggested by the apparent absence of a *shd* orthologue and thus, the lack of the last step for catalysis of ecdysone into 20E, which is generally accepted as its biologically active derivative (Campli et al. 2024). Beyond the variations in hormone synthesis pathways, the main response mechanisms to hormonal signalling might be even further remodelled. *A. syriacus* also appears to lack orthologues of the transcription factor encoding *Ecdysone-inducible protein 74* (E74) gene, which is activated early in the moulting cascade by 20E stimulation even in chelicerates. Additionally, *Kr-h1*, an important JH transducer, is also missing from the millipede genome. The responsiveness of Kr-h1 to sesquiterpenoids has only been studied in Hexapoda, but the gene is also detected in some chelicerates (Campli et al. 2024). The future availability of additional annotated genomes for millipedes will help to clarify these initial observations from *A. syriacus*.

The centipede *S. coleoptrata* displays another putative metabolic difference, where the *nvd* orthologue has presumably been lost (Figure 3). Since *nvd* encodes the enzyme catalysing the first step in the biosynthetic pathway beginning with cholesterol, its absence suggests the possibility of novel solutions for cholesterol intake. If confirmed, this would be specific to the subclass Notostigmophora, since *nvd* is found in the genomes of the centipedes *S. cingulata* and *S. maritima*, which both belong to the sister subclass Pleurostigmophora (Schumann et al. 2018). Additionally, four putative copies of the torso receptor were found in the centipede *S. coleoptrata*, but no homologues were detected in *S. cingulata* or *A. syriacus*, as previously observed in the centipede *S. maritima* (Chipman et al. 2014). Its absence might indicate deep differences not only for the regulation of the moulting process, but also for the embryonic terminal patterning, since torso binds both the paralogues prothoracicotropic hormone (PPTH) and the trunk ligand in insects (Rewitz et al. 2009; de Oliveira et al. 2019; Campli et al. 2024).

Ancestral state reconstructions map gene gain and loss events and protein domain rearrangements

While gene copy-number profiling characterises the stable and dynamic components of the moulting machinery from the perspective of extant species' gene repertoires, understanding where and when key changes may have occurred requires reconstructing gene evolutionary histories. These histories are governed by mechanisms of protein-coding gene evolution including gene duplications, losses, and more rarely *de novo* gene birth, on which evolutionary forces act resulting in modifications to the repertoire of organismal functions, and eventually the phenotype (Thomas et al. 2020). Functional innovations can arise not only from gene family expansions and contractions, but also from changes in the functional units of proteins, i.e. the gain, loss, and rearrangement of domains within the protein (Lees et al. 2016). Employing ancestral state reconstructions of gene counts and ancestral domain architectures (see Materials and Methods) the orthology dataset was analysed to trace gene family expansions and contractions across the arthropod phylogeny, and to infer domain architecture rearrangements that occurred throughout the evolution of Mandibulata.

Tracing of the evolutionary histories of gene gains and losses across Arthropoda was performed on a subset of 97 species after reducing the numbers of insects and selecting one representative for genera that included more than one species in the 145-species dataset. In total, the analysed gene families involved in moulting were predicted to have undergone 1'114 expansions and 964 contractions. Comparing across all gene families of the same age, 16.7% of ancestral nodes had a significant odds ratio for families involved in moulting processes having experienced a greater proportion of expansions (Figure 4A). That is, the odds of experiencing expansions rather than no-change or contraction events were greater for moulting-related genes than other gene families at these 16 ancestral nodes. This expansion excess amongst moulting-related gene families is evident at the LCA of each subphylum except Myriapoda, and occurs at other ancient nodes such as the Collembola LCA, the Acariformes LCA, and the ancestor of Araneae and Scorpiones. These observations point towards gene duplications playing a role in shaping the evolutionary trajectories of members of the moulting toolkit during the early diversification of the main Chelicerata lineages and the early pancrustacean radiations. No expansion excess was detected for Myriapoda, which could suggest a more stable evolutionary history in this lineage, however, better taxonomic representation is required to confirm this trend. Notably, across the represented eumetabolous insects (Holometabola and Paraneoptera) none of the 35 ancestral nodes show any significant expansion excess (Figure 4A), suggesting that gene

duplications of the moulting machinery were limited following the transition towards insect metamorphosis.

Domain architecture analysis of proteins from the 145-species Arthropoda LCA orthology dataset annotated with PfamScan catalogued an expected majority of 90% stable and maintained arrangements (Supplementary Figure 8). Amongst the identified rearrangements, 459 (44%) can be explained with exact and non-ambiguous solutions for classification as fissions, fusions, single domain emergence or loss events, and terminal emergence or loss events (Figure 4B). Compared to the events resolved across all other genes families, the moulting gene set experienced a similar proportion of fission events alongside a greatly reduced proportion of domain fusion events (15.25%, odds ratio = 0.3, -log(p.adj) = 66), i.e. a tendency to avoid creating new combinations of domains throughout their evolutionary histories. While the proportions of single domain losses are similar, the emergence of single domains is significantly higher amongst the moulting gene set members (1.31%, odds ratio = 4.6, -log(p.adj) = 7), albeit representing a small fraction of the total events. In contrast, terminal loss and emergence events are both significantly enriched for the moulting machinery with an increased proportion of terminal losses (34.42%, odds ratio = 1.6, -log(p.adj) = 12) and a large increase in the proportion of terminal emergences (8.93%, odds ratio = 25, -log(p.adj) = 100). The over-representation of gains or losses of domains at either end of an ancestral domain architecture amongst the moulting gene set members suggests a flexibility to elaborate on a conserved core, with likely functional consequences across different arthropod lineages.

Reconciliations pinpoint ancient duplications and genome screening corroborates lineage-wide losses

The copy-number profiling and ancestral state reconstructions highlight several components of the moulting machinery with evolutionary histories comprising likely ancient and maintained gene duplication events as well as potentially lineage-wide losses of otherwise widely present gene families. These events are of particular interest as they represent changes that could have substantially impacted the functional modules governing the moulting process. Potential ancient duplications were therefore carefully examined employing gene-tree species-tree reconciliation approaches, where feasible, to complement and support the inferences from ancestral state reconstructions. It is increasingly appreciated that in addition to gene duplications, gene losses can represent a mechanism

that generates genetic diversity driving lineage-specific evolution and adaptive phenotypic diversity (Albalat & Cañestro 2016; Fernández & Gabaldón 2020). Taking advantage of publicly available unannotated assemblies to predict specific sets of genes is a strategy which fully exploits an increasing amount of data generated from understudied species (Langschied et al. 2024). To corroborate potential lineage-wide losses, gene searches were performed using genomes for species from clades where orthologues appeared to be missing, and for which at least several assemblies were publicly available for representative species from the clade. These investigations focused on the chitin deacetylase (CDA) genes *serpentine* (*serp*), *vermiform* (*verm*), and *Chitin deacetylase-like 4* (*Cda4*), the chitin synthase (CHS) genes *krotzkopf verkehrt* (*kkv*) and *Chitin synthase 2* (*Chs2*), the cuticle organising *knickkopf* (*knk*) gene, a set of genes encoding prophenoloxidases, the larval stage maintaining *chinmo* gene, the adulthood determinant *E93* gene, and the Rieske-type oxygenase encoded by the *neverland* (*nvd*) gene.

The chitin deacetylases and the chitin synthases are key effectors involved in chitin fibre formation that form a major structural component of arthropod exoskeletons. The cuticle is a complex multi-layer structure where proper orientation of individual chitin fibres is fundamental to achieve a helicoidal super-organisation, mainly responsible for the overall exoskeleton resistance (Roer et al. 2015; Politi et al. 2021). In insects, the exoskeleton is built by formation of the apolysial space from its innermost edge, the endocuticle (Moussian 2010). There, a monolayer of epidermic cells produces chitin, which is then transported to the apical membrane, secreted, and assembled into the extracellular matrix. Chitin is made either by *de novo* synthesis from trehalose, mediated by chitin synthases 1 and 2 (*Chs*, *Chs1/kkv* and *Chs2*) or by recycling of the former fibres into chitin monomers, digested by Chitinases (*Chts*) and deacetylated by Chitin deacetylases (CDAs, *CDA1/serp* and *CDA2/verm*). After extrusion, chitin binds cuticle organisation and maturation effectors such as the GPI-anchored protein Knickkopf (*knk*) and arranges into organised sheets.

Reconciliation analysis of these key factors for exoskeleton remodelling identifies duplications at the LCAs of Mandibulata, Araneae, Chelicerata, and Pancrustacea (Figure 5A). The inclusion of myriapods in the dataset pinpoints the duplication of the single ancestral *CDA1/serp-CDA2/verm* chitin deacetylase gene to the Mandibulata LCA, with both copies well-maintained across the descendant lineages (Supplementary Figure 9). An independent duplication of *CDA1/serp-CDA2/verm* is also evident at the LCA of spiders, with two copies maintained in each of the five species included in the analysis. The spider LCA is also the location of the duplication of *Cda4*, another chitin deacetylase gene gain which is also maintained across the five species (Supplementary Figure 10). Both the chitin

synthases *kkv* and *Chs2* are widely present across Pancrustacea species and chelicerates also harbour generally two copies, it could therefore be assumed that both these genes were present in the Arthropoda LCA. However, the myriapods have only one copy and the reconciliation instead favours the evolutionary scenario of two independent ancestral duplications, one at the Chelicerata LCA and the other at the Pancrustacea LCA (Supplementary Figure 11). In the case of the *knk* gene family the orthology dataset identifies more than two copies in all but two of the 35 orders, suggesting the possibility of multiple ancestral duplications. The reconciliation analysis instead confirms the presence of three copper-dependent monooxygenase homologues in the arthropod ancestor, where the family is characterised by differential gene losses rather than ancient gains (Supplementary Figure 12).

The Mandibulata LCA gene gain event leading to the *CDA1/serp-CDA2/verm* pair of chitin deacetylase genes represents a likely case of functional specialisation after duplication. Both the CDA1/serp and the CDA2/verm proteins, as well as the proteins from the chelicerates, display a PFAM domain architecture that starts with an N-terminal chitin binding Peritrophin-A domain (PF01607) followed by a low-density lipoprotein receptor domain class A (PF00057). However, a C-terminal NodB polysaccharide deacetylase domain (PF01522) is only identified in the chelicerate and CDA1/serp proteins and the myriapod CDA2/verm proteins, despite the pancrustacean CDA2/verm proteins having similar protein lengths of approximately 540 to 550 amino acids (Supplementary Figure 13). Conserved Domain Database (CDD) and SUPERFAMILY domain annotations reveal a CDA-like domain spanning this region even in the pancrustacean CDA2/verm proteins, indicating that it is still generally recognisable while not specifically identified by the PF01522 profile. The CDD annotations reveal a key difference: within the CDA-like domain of the chelicerate and CDA1/serp proteins and the myriapod CDA2/verm proteins is a Zn-binding site with a conserved Asp-His-His triad, this conserved feature residue pattern is not identified in the pancrustacean CDA2/verm proteins. This suggests that after the duplication event in the Mandibulata LCA, the capacity to bind Zn was maintained in both copies in myriapods but lost in the CDA2/verm copy in the pancrustacean ancestor. CDA2/verm catalytic activity has been challenged in a few species, such as *D. melanogaster, L. migratoria*, and the prawn, *P. monodon*, where a role in mediating chitin fiber organisation has been suggested instead (Dixit et al. 2008; Sarmiento et al. 2016; Min Zhang et al. 2019; Zhang et al. 2021). Therefore, CDA2/verm might have functionally diverged from CDA1/serp and additional experimental evidence may further support an evolutionary scenario of duplication followed by functional specialisation. The pair of *CDA1/serp-CDA2/verm* genes display a highly constrained genomic organisation as their tandem position as neighbouring genes is

conserved in 65% of pancrustaceans with chromosome-level genome assemblies (and as near-neighbours allowing +/- 5 genes in 88%). Thus despite their putative functional divergence, the constraints limiting genomic rearrangements that would separate these two genes suggest that coordinated transcriptional control has played an important role in their evolutionary histories.

Amongst the losses highlighted by the gene copy-number profiling, the pro-phenoloxidases (PPOs) appeared to be absent from several crustacean orders as well as arachnid Acariformes and Sarcoptiformes (Supplementary Figure 7). PPOs encode the precursor zymogens that are activated via proteolytic cleavage to form the phenoloxidases that catalyse catechol oxidation as part of sclerotization and melanisation mediating cuticle hardening. These enzymes exhibit a complex evolutionary history and are related to the oxygen-carrying hemocyanins and the hexamerin storage proteins of insects and crustaceans (Burmester 2002; Rehm et al. 2012; Scherbaum et al. 2018). Loss patterns across Crustacea suggest multiple independent losses in Podocopida (ostracods), Harpacticoida (copepods), and the Pollicipedomorpha-Balanomorpha (barnacles) ancestor, however genomic sampling of these lineages remains too limited to test for lineage-wide losses. The arachnids, however, are better represented with available genome assemblies, and no PPO-like or hemocyanin-like genes could be recovered in any tick or mite species nor in any other Arachnida lineages (83 species) other than Araneae and Scorpiones. Therefore, across Chelicerata, while Tetrapulmonata species and horseshoe crabs might potentially rely on phenoloxidase activity, other lineages likely employ mechanisms different from catechol oxidation for mediating cuticle hardening.

In a few model insects, there is recent evidence for an important role of chinmo as a gatekeeper of the immature phenotype (Campli et al. 2024). While chinmo was identified in the orthology dataset in all hexapod orders except Odonata (Supplementary Figure 5), a putative orthologue was identified in only a single non-hexapod species, the copepod *T. californicus*. Using the *D. melanogaster* protein sequence as the search seed failed to identify any candidate orthologues in non-hexapod genomes (Crustacea: n=63, Myriapoda: n=18, Chelicerata: n=118). However, as well as the BTB/POZ (broad complex Tramtrack bric-a-brac/Pox virus and zinc finger) transcription factor domain chinmo also comprises stretches of intrinsically disordered regions that can hinder effective sequence searches. Using the *T. californicus* sequence to search non-hexapod genomes identified putative orthologues, that form best reciprocal hits to the query sequence and can be annotated with both the BTB/POZ and double zinc finger domains, in seven out of eight copepods. This tentatively dates the emergence of chinmo to the copepod-hexapod LCA, with subsequent

losses in other crustaceans. Whether these genes play analogous gatekeeper roles in copepods remains to be determined through future experimental characterisations.

While the DNA-binding E93 protein has been established as a gatekeeper of metamorphosis and adulthood fate (Ureña et al. 2016), phylogenetic profiling indicates its near-universal single-copy presence across arthropod orders and further suggests losses from multiple species characterised by direct development from the class Branchiopoda and the order Sarcoptiformes (Supplementary Figure 5). Genome searches using E93 from *D. melanogaster* or orthologues from the decapod *P. monodon* and amphipod *H. azteca* revealed no candidate E93 orthologues in any Anostraca, Diplostraca, or Notostraca crustacean order from the class Branchiopoda (22 species). For the Sarcoptiformes, only one out of the seven species in the orthology dataset harboured a putative E93 orthologue. These widespread losses were further supported by genome searches with sequences from the spider *P. tepidariorum* and the mite *T. urticae* that recovered putative E93 orthologues in only 28% of the examined Sarcoptiformes (16/57 species). These lineage-specific independent losses of E93 across different subphyla may have played a role in the regulatory rewiring of toolkit components controlling the progression of development through progressive moults.

The Rieske monooxygenase encoded by the gene *neverland* (*nvd*) was near-universally present across the orders represented in the orthology dataset, yet no copies were found for Coleoptera or Mesotigmata, which are represented by 11 and four species, respectively (Supplementary Figure 2). Extensive searches of available genomes failed to reliably predict copies of the *nvd* gene in any of the 251 assemblies for Coleoptera, spanning 41 different taxonomic families, or any of the seven Mesostigmata species with available assemblies. For beetles this presents a strong case for the order-wide loss of *nvd* in the coleopteran ancestor, while within Mesostigmata additional representative species are needed to confirm this potential loss and if confirmed, to better understand its extent. The genome searches of the seven Mesostigmata species using the *nvd* protein sequences from the spider *P. tepidarioum* and the mite *T. urticae* returned no reliable gene predictions. While the orthology dataset identified no beetle orthologues, the genome searches using the *nvd* gene from *D. melanogaster* as the search-seed returned three potential hits in *Anisosticta novemdecimpunctata* (Coccinellidae, ladybirds), *Liopterus haemorrhoidalis* (Dytiscidae, diving beetles), and *Sceptobius lativentris* (Staphylidae, rove beetles), and using the *nvd* gene from *A. mellifera* (Hymenoptera) as the search-seed identified two hits within the Chrysomelidae family of leaf beetles, in *Octodonta nipae* and *Galerucella tenella* .

The predictions from the assemblies of *A. novemdecimpunctata*, *L. haemorrhoidalis*, had low sequence similarity to any arthropod protein (*D. melanogaster* and *A. mellifera* included) and showed no domain annotations expected of *nvd* orthologues. The candidate *S. lativentris nvd* gene is found on an 1258 bp contig and the protein exhibits the characteristic Rieske domain, however, the sequence is almost identical to a protein from the Sarcoptiformes mite, *Tyrophagus putrescentiae* (99%). Originally thought to be mycetophagous, this mite feeds on insects including coleopterans such as the tobacco beetle *Lasioderma serricorne* (Papadopoulou 2006), suggesting that mite tissue may have been present in the sample used to sequence the *S. lativentris* genome. The *O. nipae* candidate also exhibits the expected domains, however, it shows greatest sequence identity (>50%) with nvd proteins from Sarcoptiformes mites. The candidate *G. tenella nvd* gene is found on an 88 Kbp contig and the protein exhibits the characteristic Rieske domain, however, it has greatest sequence identity with proteins from the endoparasitoid wasps *Microctonus hyperodae* (66%) and *M. aethiopoides* (59%). Endoparasitoids of the genus *Microctonus* are known to target beetle hosts from the Chrysomelidae family such as cabbage stem flea beetle, *Psylliodes chrysocephala* (Jordan et al. 2020), indicating that the sample used to sequence the *G. tenella* genome may have been harbouring wasp eggs or larvae.

The low-identity hits without Rieske domains are likely spurious predictions and the other *nvd* gene predictions probably represent sample contaminations with plausible biological explanations. Therefore, taking into account the extensive genome sampling across Coleoptera, the evidence suggests that the beetle ancestor likely lost the *nvd* gene encoding the key ecdysteroid pathway Rieske monooxygenase. Based on current biochemical knowledge, loss of the enzyme probably also indicates loss of the ability to transform cholesterol into 7-dehydrocholesterol. No other protein capable of catalysing this reaction (EC:1.14.19.21) was found in beetles, when querying the ENZYME database (Release 24/07/2024) and UniProtKB, even including those with an unreviewed status (Bairoch 2000). Furthermore, no enzyme was identified in beetles when considering the reverse catalytic reaction known from the mammalian DHCR7 reductase (EC:1.3.1.21), which mediates the last step of cholesterol synthesis. Similarly for Mesostigmata, searching for proteins putatively capable of catalysing these reactions returned no candidates for any hypothetical functional replacements. Known from studies in model insects, nvd is localised in the endoplasmic reticulum and its catalytic activity depends on the Rieske [2Fe-2S] motif within the Rieske domain (Interpro entry IPR017941) (Yoshiyama-Yanagawa et al. 2011; Pan et al. 2021). Beetles do possess other genes encoding proteins with this key domain, such as a Cytochrome b-c1 complex subunit located in the mitochondrial inner membrane mediating electron transport (EC:7.1.1.8), and an apoptosis-inducing factor 3 protein with a cytoplasmic

localisation. However, the 3-ketosteroid-9-alpha-monooxygenase-like C-terminal domain (Interpro IPR045605) that follows the Rieske domain of the nvd protein, is not detectable in any beetle protein based searches of the Interpro and UniProt databases.

Cuticle protein repertoire dynamics vary across arthropod subphyla

The exoskeleton represents a hallmark structure essential to all arthropods that provides physical support and resistance to mechanical and chemical stress, with variations in the structural arrangement of layers and different chemical compositions (Roer et al. 2015; Hensel et al. 2016; Politi et al. 2021; Bello et al. 2022). Exoskeleton assembly and remodelling relies on the building blocks of chitin polymers and CPs, where the superfamily of CP genes is known for its large size and complex evolutionary history (Willis 2010). Therefore, CP gene repertoires were examined by identifying canonical CPs within the annotated proteome of each species based on the presence of their representative Rebers and Riddiford (RR) chitin binding domain (Pfam domain PF00379) (Moussian 2010; Willis 2010; Roer et al. 2015; Mrak et al. 2017). As a key component of the biophysical interface between the arthropod and its immediate environment, the physico-chemical properties (Osorio et al. 2015) of CP repertoire amino acid sequences were also characterised to investigate differences across subphyla.

The species with the smallest CP repertoires included *A. nasatum* (Isopoda, Crustacea), and *S. scabiei, H. destructor, O. nova, D. farinae, B. tropicalis*, and *D. pteronyssinus* (Acariformes, Chelicerata) with 19 to 25 genes, while the largest by far were the three *Penaeus* crustaceans. Comparing across subphyla shows that crustaceans harbour, on average, a significantly larger repertoire of CPs, which varies greatly from as few as 19 from *A. nasatum* to more than 600 genes from *P. monodon*, *P. vannamei*, and *P. chinensis*, and a median of 212 CPs (Figure 6A). Median counts for Hexapoda (87), Myriapoda (34), and Chelicerata (70) are all much lower, and they show less within-subphylum variation than the crustaceans. To examine whether larger repertoires necessarily mean more diverse repertoires, proteins from each species with sequence similarities of 80% or more were clustered together. The ratio of clusters to counts is a proxy for CP repertoire redundancy, with lower values indicating the presence of more sets of similar CPs. This shows that despite the large counts in many crustaceans, these CPs are often similar in sequence and therefore do not represent more diverse repertoires (Figure 6B).

Examining their physico-chemical properties revealed that crustacean and hexapod CPs are characterised by the lowest predicted isoelectric point (pI) values, contrasting Pancrustacea with the higher values in Myriapoda and Chelicerata (Figure 6C). High-pI CPs are more basic and bind to negatively charged chitin forming more rigid cuticles, while low-pI CPs are more acidic and help buffer pH, regulate hydration, or interact with positive ions resulting in softer or more flexible cuticles. Acidification below the pI might weaken inter-protein interactions promoting elastic and plastic stretch, suggesting that lower pI values in Pancrustacea may facilitate cuticle expansion capacities (Reynolds 1975; Benoit & Denlinger 2010; Flynn & Kaufman 2015). The CP aliphatic index, where higher values indicate greater proportions of nonpolar amino acids, shows a different contrast among the subphyla, with the highest average values in hexapods, albeit with a wide range across species (Figure 6C). Proteins with an elevated aliphatic index are more hydrophobic and generally more heat-resistant, suggesting that the CP repertoires in many hexapods and some chelicerates are compositionally adapted to withstand higher temperatures. The hydrophobic moment index, where high values indicate clustering of hydrophobic residues to present a clearly defined hydrophobic face and low values mean the residues are evenly spread, is elevated in Chelicerata compared to the three mandibulate subphyla (Figure 6C). As CPs are anchored in a complex matrix containing chitin, other CPs, lipids, cross-linking agents, etc. their hydrophobic moment influences how they are positioned within the matrix and how they interact with other components (Moussian 2013). Low-moment CPs do not have distinct hydrophobic and hydrophilic faces and thus require higher levels of covalent sclerotisation for structural integrity while high-moment CPs may function in anchoring or organising cuticle layers. This suggests that in chelicerates the particular CP localisation and orientation in the extracellular space within the cuticular matrix may be functionally relevant (Politi et al. 2021). Taken together, these results demonstrate that CP repertoires and properties vary across major arthropod groups and likely reflect different evolutionary routes, enabling hypothesis generation about order-specific mechanisms in aquatic Crustacea and adaptation to life on land in Hexapoda and Chelicerata (van Straalen 2021).

Discussion

The broad taxonomic sampling across 35 arthropod orders, including three newly sequenced and annotated myriapods, enables the examination of moulting gene repertoire evolution in deep time with fine granularity. Genomic surveying and gene copy-number profiling

highlights the ancient origin of the moulting machinery toolkit, with overall lower levels of protein sequence divergence, and with contrasting stable and dynamic components from across the six functional modules governing moulting processes. The presence of the toolkit in the arthropod LCA is supported by previous studies focused on limited subsets of moulting-related genes describing the ancient origins of key ligand-receptor components (de Oliveira et al. 2019), members of the sesquiterpenoid and ecdysteroid pathways (Qu et al. 2015), the so-called “Halloween genes” (Schumann et al. 2018), or enzymes involved in the final steps of JH synthesis (Smykal & Dolezel 2023). Reconstructing ancestral gene contents across arthropods reveals numerous gain and loss events, with moulting-related gene families experiencing elevated expansions at ancient nodes of the phylogeny. This contrasts the moulting gene repertoire with global gene content evolution where previous arthropod-wide (76 species) gene content analyses pointed to relatively evenly distributed rates of duplications and losses (Thomas et al. 2020). Gene duplications therefore appear to have played an important role in shaping the ancestral moulting machinery, followed by more stable evolutionary trajectories in younger lineages. Stable too are the majority of protein domain architectures, except for an over-representation of terminal loss or emergence events amongst the moulting gene set members that could suggest functional elaborations. The conserved and ancient core is nevertheless characterised by dynamic gene repertoire changes observed across all six moulting modules and nearly all 35 examined orders, with the ecdysteroid pathway and late genes showing elevated proportions of duplications. Indeed, global analyses previously identified ecdysteroid metabolism genes amongst the most dynamically changing arthropod gene families, alongside xenobiotic defence, digestion, chemosensation, chitin metabolism, and others (Thomas et al. 2020). Complementing phylogenetic profiling with ancestral state reconstructions of gene contents and protein domain architectures provides a robust approach to characterise the evolutionary dynamics of the arthropod moulting machinery.

One limitation to the characterisation of such patterns is where orders are represented by a single species (43%) or only two species (9%). The lack of “replicates” means that estimates are based on only one or two species, which may not be representative of the order as a whole and may inflate inferred gains or losses. Higher copy-numbers observed in some of these lineages could nevertheless reflect true gene gains, possibly arising from whole genome duplications (WGDs), e.g. in Xiphosura horseshoe crabs with three WGDs (Nong et al. 2021), or the WGD event in Balanomorpha and Pollicipedomorpha barnacles (Jee-Hoon Kim et al. 2019; Bernot et al. 2022; Yuan et al. 2024), or high duplication levels reported for the Siphonaptera cat flea, *C. felis* (Driscoll et al. 2020; Feyereisen 2022). Assertions of gene losses across the arthropod phylogeny are particularly challenging in lineages where species

representation is limited. For example, the Isopoda representative *A. nasatum* appears to lack several key moulting machinery components, but its genome annotation may be incomplete, so comparisons with other isopods are needed. Where multiple additional unannotated assemblies for a clade are available, targeted genome screening can provide the support needed to corroborate lineage-wide losses, such as the remarkable absence of *nvd* across Coleoptera. Fortunately, ongoing assembly and annotation of genomes from across the tree of life (Mazzoni et al. 2023; Blaxter et al. 2025) will enable future rigorous evaluations of such putative losses of key members of the moulting gene repertoire. This will need to be accompanied by experimental studies across Arthropoda, to verify functional hypotheses based on phylogenomic comparisons, and to identify new components of the moulting machinery that may be specific to less well studied clades.

The moulting gene repertoire includes both predominantly single-copy and predominantly multi-copy families, reflecting genome-wide patterns in which constrained single-copy genes contrast with relaxed multi-copy families (Waterhouse et al. 2011). Additionally, there are numerous lineage-specific elaborations in the form of gene duplications maintained across descendant lineages (with or without subsequent protein domain changes), and lineage-wide losses of otherwise widely maintained genes. These lineage-specific elaborations, and the capacity for lineage-specific changes in multi-copy families, are likely to be directly or indirectly linked to differences in the variety of life histories across arthropod diversity, with key factors being dietary physiology, developmental modes, and environmental constraints. With respect to diet, highly variable steroid composition from different food sources might promote diversification of organismal capabilities for hormone biosynthesis with implications for how moulting processes are regulated. This is supported by experimental evidence of a heterogeneous cocktail of ecdysteroid intermediates and analogues in different lineages that are able to elicit moult-inducing biological responses (Campli et al. 2024). For instance, instead of the insect 20-hydroxyecdysone (20E), ponasterone A (25-deoxy-20E) has been suggested as a major bioactive ecdysteroid in some Crustacea and Chelicerata lineages. For growth and development, moulting and post-embryonic development are inextricably linked because moulting is both the mechanism that makes growth possible and the process that enables developmental transitions. These transitions may be direct and gradual or indirect and metamorphic, gradual developers require moults that preserve functional continuity and implement small incremental morphological changes, whereas metamorphic developers rely on hormonally distinct moults that coordinate large-scale remodelling, enabling transitions between ecologically and morphologically disparate life stages. In contrast to diet and development, environmental constraints may manifest more prominently in variations of the structural components of the moulting machinery rather than through

regulatory changes. Here the same underlying exoskeleton renewal process is expected to reflect adaptations to marine and freshwater habitats as well as terrestrialisation events, semi-aquatic life histories, and the innovation of insect flight (Asano et al. 2019; van Straalen 2021; Vargas et al. 2021; McNamara & Freire 2022). These and other questions remain to be explored, nonetheless, our phylogenetically broad and deep analyses of the major components involved in moulting reveal under-appreciated evolutionary dynamics, with the arthropod moulting machinery showing developmental flexibility by accommodating lineage and functional variability, within a framework of conserved molecular modules and phenotypic outcomes (True & Haag 2001; McColgan & DiFrisco 2024).

Materials and Methods

Myriapod sample collection, DNA and RNA sequencing

Animals were collected between February and April 2022-2023 in the Givat HaArbaa, Jerusalem, Israel (GPS coordinates: 31°44′00″N 35°12′48″E). *Scolopendra cingulata* and *Scutigera coleoptrata* were kept in individual transparent plastic boxes with a substrate and large pieces of bark and fed weekly with *Blattella germanica* nymphs. *Archispirostreptus syriacus* individuals were kept together in a large transparent plastic container filled with substrate and egg cartons and were fed weekly with small pieces of vegetables. The substrate was obtained from the collection site. Animals were kept in a climate-controlled room with the following set parameters: temperature (25 ± 1°C), humidity (~ 40%), and light:darkness regime (14h:10h). Additionally, the substrate was moistened weekly with double-distilled water. No special approvals, such as ethical or collection permits, were required for handling these species. The genomic vouchers are deposited in The National Nature Collections, The Hebrew University of Jerusalem under the following museum voucher numbers: HUJ-INV-CHIL764 (*S. cingulata*), HUJ-INV-CHIL763 (*S. coleoptrata*), HUJ-INV-DIP113 (female *A. syriacus*), and HUJ-INV-DIP114 (male *A. syriacus*).

Animals were anesthetised using carbon dioxide inhalations. Substrate particles were gently removed by washing with molecular biology-grade water. Animals were dissected, flash-frozen in liquid nitrogen, and ground into powder using a mortar and pestle. The DNA sample of *S. cingulata* was obtained from the head and several anterior body segments of the female individual. The gut was dissected out before flash-freezing to minimise bacterial contamination. The whole-body sample, excluding the gut, was used to extract the DNA sample of female *S. coleoptrata* specimen. The genome assembly of *A. syriacus* is based on two independent DNA extractions and sequencing procedures, one was obtained from the head and several anterior trunk segments of the female individual, and another sample was derived from the trunk segments of the male. The gut and legs were excluded from the extraction reaction in both cases. The optimal tissue amount for each species was determined experimentally and proved to be a crucial factor in the successful extraction of long DNA fragments. DNA extraction and RNAse treatment were performed using Monarch Genomic DNA Purification Kit (New England Biolabs). The samples of *S. cingulata* and *S. coleoptrata* were extracted following the manufacturer's protocol. The body *A. syriacus* has a well-developed parietal fat body which complicates the extraction of clean DNA samples, requiring a modified protocol. After the lysis reaction and centrifugation, the supernatant was

slowly mixed with phenol:chloroform;isoamyl alcohol (25:24:1) saturated with 10 mM Tris, pH 8.0, 1 mM EDTA (Sigma) for 3 hours, and the DNA from the aqueous phase was then precipitated with ethanol to obtain a crude DNA sample. This sample was used for RNase treatment and column purification, following the manufacturer's protocol. The purity and the concentration of DNA samples were assessed using NanoDrop 1000 (Thermo Fisher Scientific), the concentration was additionally confirmed on Qubit Flex Fluorometer using Qubit 1X dsDNA HS Assay Kit (Thermo Fisher Scientific). Samples were stored at -80ºC and transported in dry ice to the Lausanne Genomic Technologies Facility for further processing. 5200 Fragment Analyzer system (Agilent) was used to evaluate the fragmentation level of the samples. For the genome annotation, RNA was extracted from several body parts, including whole-body samples without gut, head, ovaries, and testicles. The Quick-RNA MiniPrep Kit (Zymo Research, R1055) was used for RNA extraction, following the manufacturer's instructions. The purity and the concentration of the obtained RNA samples were estimated with NanoDrop 1000 (Thermo Fisher Scientific). RNA integrity was analysed using a Bioanalyzer system (Eukaryote Total RNA Nano kit, Agilent). RNA libraries were prepared using Illumina Stranded mRNA Prep kit and sequenced on a PE150 AVITI (Element Biosciences) at the Lausanne Genomic Technologies Facility.

Myriapod genome assembly and annotation

High-quality genomic DNA was sequenced using PacBio HiFi sequencing on a PACMAN instrument, generating highly accurate long reads. The sequencing coverage was approximately 46× for *S. cingulata*, 40× for *S. coleoptrata*, and 30× for *A. syriacus*. The quality of the reads was assessed using LongQC (v1.2.0c) (Fukasawa et al. 2020), while genome characteristics, including ploidy and heterozygosity, were estimated using Smudgeplot (v0.2.5) and GenomeScope2 (v2.0) (Ranallo-Benavidez et al. 2020). Genome assembly was performed using Hifiasm (v0.19.2) (Cheng et al. 2021) and/or Purge_dups (v1.2.6) (Guan et al. 2020), applying different purging strategies depending on the species. For *S. cingulata*, assembly was performed exclusively with Hifiasm using its strongest purging level (-l3). For *A. syriacus* and *S. coleoptrata*, Hifiasm was first applied with the strongest purging setting (-l3) and further refined using Purge_dups. Assembled genomes were screened for contaminants using fcs_gx (v0.5.0) (Astashyn et al. 2024) before final quality assessment. Genome completeness and accuracy were evaluated using the Benchmarking Universal Single-Copy Orthologues (BUSCO) (v5.4.3) assessment tool with the arthropoda_odb10 database (Manni et al. 2021). Additional assembly statistics were obtained using gfastats (v1.3.6) (Formenti et al. 2022), and k-mer-based quality assessment was performed using Merqury (v1.3) (Rhie et al. 2020). The genome assemblies exhibited

high completeness and contiguity, with BUSCO scores and N50 values reflecting well-assembled genomes across all three species. The *S. cingulata* assembly is composed of 600 contigs, an N50 of 63,664,107 bp, and a BUSCO completeness of C:97.6% [S:95.2%, D:2.4%], F:0.2%, M:2.2%, n:1013. *S. coleoptrata* was assembled into 344 contigs, with an N50 of 20,554,343 bp and BUSCO scores of C:97.1% [S:96.1%, D:1.0%], F:1.2%, M:1.7%, n:1013. The *A. syriacus* assembly contained 3,887 contigs, with an N50 of 1,010,713 bp and BUSCO completeness of C:96.5% [S:94.2%, D:2.3%], F:1.8%, M:1.7%, n:1013.

Genome annotation was performed by first identifying repetitive elements using RepeatModeler (v2.0.4) (Flynn et al. 2020). Protein-like transposable elements (TEs) were filtered out using BLAST (v2.7.1) (Camacho et al. 2009), transposonPSI (v1.0.0) and ProtExcluder (v1.2) (Campbell et al. 2014). The remaining repetitive elements were then masked in the genome using RepeatMasker (v4.1.5) (Smit et al. 2013). To facilitate gene prediction, RNA-seq data were generated for each species and supplemented with publicly available datasets from the Sequence Read Archive (SRA). For *S. cingulata* and *A. syriacus*, RNA was extracted from an adult female's head and a few anterior body rings, excluding the gut. For *S. coleoptrata*, RNA was extracted from the whole body of an adult female, also excluding the gut. The RNA samples were sequenced using the Illumina NovaSeq platform, generating strand-specific mRNA libraries with paired-end reads. To enhance the comprehensiveness of the transcriptome data, publicly available RNA-seq datasets from SRA were also used. For *S. cingulata*, SRR1653235 was included, which contains RNA extracted from the anterior half of the trunk, excluding the head and poison claws. For *S. coleoptrata* these included, SRR1653237, derived from a whole organism excluding the head and poison claw, SRR8998264, extracted from the forcipule, and SRR1158078, for which the tissue of origin is unknown. RNA-seq data quality was assessed with FastQC (v0.12.1) (Andrews 2010), and sequencing adaptors and low-quality reads were removed using Atropos (v1.1.28) (Didion et al. 2017). The filtered RNA-seq reads were aligned to the genome using HISAT2 (v2.2.1) (Daehwan Kim et al. 2019), and mapping statistics were generated using SAMtools (v1.17) (Li et al. 2009) and QualiMap (v2.2.2d) (Okonechnikov et al. 2016). Protein-coding gene annotation was performed using BRAKER3 (v3.0.8) (Gabriel et al. 2023), integrating the previously aligned RNA-seq data along with curated protein evidence from OrthoDB (Tegenfeldt et al. 2025). The completeness of the predicted annotation was evaluated using BUSCO (v5.4.3), provided in Supplementary Table 1.

Publicly sourced genome assemblies and annotations

To obtain a broad representation of arthropod diversity for orthology delineation the completeness of the arthropod genome assemblies available from the United States National Center for Biotechnology Information (NCBI) was evaluated using the Arthropod Assembly Assessment Catalogue (A3Cat, release 2024-07-01) (Feron & Waterhouse 2022a). Assemblies were required to have an annotated proteome with the number protein-coding genes ranging from 8’000 to 50’000. These were then filtered based on the A3Cat BUSCO scores: the annotated assembly having the highest Arthropoda Complete BUSCO score was retained where more than one assembly was available for individual species; all selected assemblies were required to have scores of less than 40% Arthropoda Duplicated BUSCO and at least 75% Arthropoda Complete BUSCO. These thresholds were applied specifically to avoid the exclusion of some non-insect arthropods from key underrepresented lineages required to ensure a broad representation of arthropod diversity. Subsequently, to produce a more balanced phylogenetic diversity, insect taxonomic orders with more than 12 species were down-sampled, by retaining within each order one representative for each taxonomic family, having the highest Arthropoda Complete BUSCO score among the species of that family. Additionally, representative species for the families Drosophilidae (Diptera), Tenebrionidae (Coleoptera), and Bombycidae (Lepidoptera) were manually selected: *D. melanogaster* (Release_6_plus_ISO1_MT), *T. castaneum* (GCF_031307605.1), and *B. mori* (GCF_030269925.1), respectively, given their well-established history as model systems and the accumulated knowledge of genes involved in moulting process. Proteomes and annotation feature tables from the selected assemblies were downloaded from NCBI repositories GenBank and RefSeq (2024-07-12) and assessed for completeness using BUSCO v5.4.3 and the arthropoda_odb10 lineage dataset (option: -mode protein) (Manni et al. 2021). All annotated proteomes with a score of at least 75% Arthropoda Complete BUSCO were retained and filtered for the protein-coding longest isoform based on their corresponding annotation feature table. This resulted in the selection of the annotated proteomes of 145 arthropod species representing 35 orders from the four major subphyla, with Arthropoda BUSCO Complete scores of median 96.2% (mean 91.4%, standard deviation 6.0%) and Arthropoda BUSCO Duplicated scores of median 1.9% (mean 3.8%, standard deviation 5.8%), and protein-coding gene counts of median 15’649 (mean 17’603, standard deviation 6’723%). Assembly accessions, protein-coding gene counts, and BUSCO assessments are provided in Supplementary Table 1.

Species phylogeny reconstruction

The species phylogeny was computed from single-copy orthologues found in at least 95% of the total set of 145 species, detected by the BUSCO assessments performed at A3Cat on

the genome assemblies using the arthropoda_odb10 lineage dataset. Protein sequences were aligned using MUSCLE v3.8.1551 (Edgar 2004) with default parameters and trimmed using the automated method for threshold optimization in TrimAl v1.4.1 (option -strictplus) (Capella-Gutiérrez et al. 2009). A concatenated super-alignment was built from the individual alignments (76’471 columns, 71’014 distinct patterns, 57’142 parsimony-informative, 9’412 singleton sites, 9’917 constant sites; other metrics computed by Alistat v1.15 (Wong et al. 2020) are available as Supplementary Table 2) for the phylogeny reconstruction performed using ModelFinder as implemented in IQ-TREE v2.2.0-beta with 1’000 ultrafast bootstrap samples (option -msub nuclear -B 1000 -bnni) (Nguyen et al. 2015; Kalyaanamoorthy et al. 2017; Hoang et al. 2018; Minh et al. 2020). The resulting phylogeny was inspected and manually rooted in NJ-plot using chelicerate species as the outgroup (Perrière & Gouy 1996). The paraphyletic crustaceans, comprising Hexapoda and Crustacea within the monophyletic Pancrustacea were recovered, whereas three orders each represented by only a single species were observed to be in disagreement with previous phylogenomics findings: placement of the horseshoe crab *L. polyphemus* (Xiphosura, Chelicerata) within Arachnida, positioning of the copepod *T. californicus* (Harpacticoida, Crustacea) as sister to species of the Branchiopoda class (namely Diplostraca and Anostraca), and the dragonfly *L. fulva* (Odonata, Hexapoda) not clustering with Ephemeroptera species. Therefore, a second round of phylogeny reconstruction in IQ-TREE was performed applying constraints to achieve the correct topology as follows: early branching of *L. polyphemus* before the Arachnida LCA, diverging of *T. californicus* from the LCA of Malacostraca and Thecostraca, and Ephemeroptera species sharing the most recent common ancestor with *L. fulva* (Misof et al. 2014; Schwentner et al. 2018; Howard et al. 2020). The molecular species tree was time-calibrated using ten calibration nodes (Supplementary Table 3), supplied to the functions makeChronosCalib() and chronos() from the ape v5.8 R package (Paradis & Schliep 2019). Divergence time estimates were sourced from the TimeTree v5 database (Kumar et al. 2022). The resulting ultrametric species phylogeny representing 600 million years of arthropod evolution with 144 internal nodes was used for ancestral state reconstructions and gene-tree-species-tree reconciliation analyses.

Orthology delineation across 145 arthropod species

Orthology was delineated at the level of the Last Common Ancestor (LCA) of all the 145 selected arthropod species, where an orthologous group (OG) represents the set of genes descended from a single gene in the arthropod LCA. OGs were reconstructed from 142 publicly available annotated proteomes and three myriapod species newly assembled and annotated in this study. The OrthoDB standalone pipeline OrthoLoger v3.0.2 was run with

default parameters (Kuznetsov et al. 2023), after filtering the proteomes for the single longest protein-coding isoform of each gene. The OrthoLoger algorithm uses all-against-all pairwise protein sequence alignments to identify best reciprocal hits (BRHs) between all genes from each species pair in the dataset. Subsequently, a graph-based clustering procedure starting with BRH triangulation progressively builds OGs aiming to identify and include all genes descended from a single gene in the LCA. The resulting orthology dataset comprised a total of 74’214 OGs and 2’047’671 genes, representing 80% of the input set of 2’552’371 genes from the annotated proteomes of 145 species. OG phyletic ages were computed as the LCA of all the species included in the OG, simplified to stratifications of Arthropoda, Mandibulata (Pancrustacea + Myriapoda), the four subphyla, and younger than subphyla. OG evolutionary rates were computed using OrthoLoger ancillary tools: pairwise protein alignments are used to calculate average of inter-species identities for each OG, normalised over the average identity of all inter-species BRH, as defined by OrthoDB (Waterhouse et al. 2013).

Identification of moulting-related genes from the orthology dataset

The lists of genes with evidence of involvement in various moulting processes was curated based on an extensive literature review of the accumulated knowledge of the genetic toolkit governing arthropod moulting (Campli et al., 2024) and manual searches of the FlyBase database (Öztürk-Çolak et al. 2024). The curated list of gene names and NCBI protein identifiers comprises primarily genes from the well-studied *D. melanogaster* fruit fly (n=74), complemented by a further 48 genes from other relatively well-studied insects *B. mori* and *T. castaneum*, decapods *L. vannamei* and *P. trituberculatus*, and the common house spider *P. tepidariorum* (Supplementary Table 4). Considering evidence from the literature, these genes collectively represent 76 moulting-related genes, or targeted gene families of interest for this genomic survey characterising the evolutionary histories of the toolkit of molecular components involved in moulting processes. The protein identifiers were collated to match the versions of the annotated proteomes used for orthology delineation so the gene lists could be used as “seeds” to search the orthology dataset and identify relevant OGs representing the gene families of interest. The dataset was manually curated to reflect current knowledge: in order to reflect the shared history of *stw* with *mco1*, and *chs2* with *kkv* (Arakane et al. 2005; Moussian 2010; Asano et al. 2019), their individual OGs were merged together, respectively. Profiling of orthologue copy-numbers per species for each gene family of interest across the main functional categories/modules and taxonomic groups was performed in R v4.3.2 and plotted using the ggplot2 package (Wickham 2016).

Gene-tree-species-tree reconciliation

The process of reconciling a gene tree with a species tree aims to map gene duplication events, gene loss events, and speciation events, given a model of gene family evolution, *i.e.* to trace the evolutionary history of a gene family. Confidence in the inferred evolutionary scenarios requires robust input gene trees, which can be challenging to achieve with large sets of diverse species. Given the focus on characterising deep-time events (*i.e.* mainly order-level and older), and that analysing fewer species produces more confident gene trees, a subsampling of the full orthology dataset was performed before gene-tree-species-tree reconciliation. For the insect orders of Diptera, Lepidoptera, Hymenoptera, Coleoptera, and Hemiptera, species sets were down-sampled by choosing for each order the subset of species having the five highest Arthropoda Complete BUSCO scores computed on the proteome. Additionally, for the other arthropod orders, where the same genus was present more than once, a single species for each genus was selected using the same criteria, overall resulting in a subsampled dataset of 97 species. The species tree used for the reconciliations was obtained by pruning the 145-species phylogeny to retain these 97 species. The gene families analysed consisted of the moulting-related genes identified from the orthology dataset. Protein sequences from each gene family were aligned using the iterative refinement L-INS-i algorithm from MAFFT v7.520 (Katoh & Standley 2013). Alignments were trimmed using TrimAl v1.4.rev15, firstly with the heuristic automatic method (option: -automated1) and further by removing fragmented protein sequences that could represent incomplete gene annotations (option -resoverlap 0.7 -seqoverlap 70) (Capella-Gutiérrez et al. 2009). Gene trees were reconstructed using maximum likelihood estimates as implemented in RAxML v8.2.12, choosing the GAMMA model and JTT substitution matrix and performing 1000 rapid bootstrap samples (option -f a -N 1000 -m PROTGAMMAJTT) (Stamatakis 2014). Gene trees were rooted in the Python ete3 module, using the chelicerate sequences as outgroup when monophyletic, otherwise when polyphyletic or not present in the tree, midpoint rooting was applied (Huerta-Cepas et al. 2016). For analysing only the most robust input gene trees, only those with more than 50% of the nodes supported by bootstrap values higher than 50% were then used for reconciliations with the species tree. Gene-tree-species-tree reconciliation was performed using the parsimony approach of NOTUNG v.2.9.1.5, under a Duplication and Loss model with default costs and allowing the rearrangement of branches at nodes with less than 90% bootstrap support (option --rearrange --threshold 90 --infertransfers false) (Stolzer et al. 2012). The summary of deep time events from selected gene families is presented in Supplementary Table 5.

Gene count ancestral state reconstruction

Ancestral state reconstruction aims to estimate the likely state (in this case gene copy numbers) at the internal nodes of the species tree given the observed state at the terminal branches and a model of gene family evolution. To estimate ancestral gene copy numbers, and thus map gene family expansion and contraction events on the species tree, a maximum likelihood approach to the birth-death model of gene family size evolutionary rate was employed, as implemented in Computational Analysis of gene Family Evolution (CAFE) v5 (Mendes et al. 2021). Firstly, the phyletic age of each OG was calculated as the LCA of all the species represented in the OG, considering the full species phylogeny. Then, only OGs with a phyletic age of Arthropoda LCA and with species included in subsampled dataset (97 species set) were used for the input gene count table provided to CAFE. Two separate sets of CAFE runs were performed, (1) for the foreground (all the proteins identified in moulting-related OGs as old as the Arthropoda LCA), and (2) for the background (all the proteins belonging to OGs as old as the Arthropoda LCA, excluding the foreground). The background was further filtered to remove gene families with more than 100 gene copies in one or more species, following CAFE guidelines (using the provided Python script, clade_and_size_filter.py). To ensure model convergence, each set was run independently four times under different parameter settings, always estimating lambda with one k rate category. For the background set, Poisson and normal root family size distributions, and different lambda rates up to four (one for each subphyla) were tested. Using the Poisson distribution and two lambda rates (one for Chelicerata and one for Mandibulata), resulted in estimation of lambda parameters respectively as 0.0017 and 0.0018, supported by a maximum likelihood score of -lnL 1.30946e+06. For the foreground set, gene count ancestral state reconstruction was performed using the output from the background set run, resulting in lambda parameter estimates of 0.0009, 0.0018 with a maximum likelihood score of -lnL 7921.63.

Protein domain evolutionary history analyses

Domain annotation of the longest protein isoforms was performed using PfamScan (Mistry et al. 2007). Consecutive repeated annotations were collapsed (i.e. A-B-B-B-C -> A-B-C) as indicated for ancestral domain rearrangement reconstruction in DomRates (Dohmen et al. 2020). Two separate runs using the set of Chelicerata species as the outgroup were performed for the foreground (all the proteins involved in the moulting process in OGs as old as the Arthropoda LCA) and the background (all the proteins belonging to OGs as old as the

Arthropoda LCA, excluding the foreground and the proteins without an ortholog), as for the ancestral state count reconstruction. Fisher tests were performed in R stats package v4.3.2 (R Core Team 2023).

Support for clade-wide gene losses using *de novo* gene finding with MetaEuk

To further assess potential gene losses observed from the proteome-based orthology analysis, the A3cat resource was used to identify genome assemblies without protein-coding annotations available from the NCBI. When multiple assemblies were available for a single species, the assembly with the highest Arthropoda Complete BUSCO score was selected. Only assemblies with at least 75% BUSCO score were retained to perform *de novo* gene finding with MetaEuk (Levy Karin et al. 2020). Genome-wide searches were carried out using the longest protein isoforms of the genes of interest (seed protein identifiers in Supplementary Table 6) as input to MetaEuk (option: --exhaustive-search).

Annotation and analysis of cuticle protein gene families

Results from PfamScan were filtered for the domain “PF00379.27” (“insect cuticle protein”, “chitin_bind_4”) to retrieve proteins annotated as canonical cuticle proteins (CPs) harbouring the Rebers and Riddiford (RR) chitin binding consensus motif, as indicated in Willis, 2010 (Willis 2010). CPs of each subtype, in each species, were clustered by 80% sequence similarity using CD-HIT (v4.8.1) (Li & Godzik 2006). Molecular properties such as aliphatic index, hydrophobic moment index, and isoelectric point of each CP were computed using the Peptides package (Osorio et al. 2015).

Data Availability

The data underlying this article are publicly available in the European Nucleotide Archive (ENA) at https://www.ebi.ac.uk/ena/browser/home and can be accessed with the accession numbers provided in Supplementary Table 1. The genome assemblies and annotations for the three myriapod species produced as part of this study are being processed for submission to the ENA.

Acknowledgements

The authors thank all members of the Sinergia project “An interdisciplinary study of arthropod moulting: linking genotype, phenotype and life history evolution” for useful discussions that supported the development of this manuscript. We are also grateful to Rosa Fernández for making available RNAseq data from *Scutigera coleoptrata* to assist with genome annotation, and to Romain Ferron for assistance with building the arthropod species phylogeny.

Funding

This work was supported by the Sinergia programme of the Swiss National Science Foundation (grant number: 198691)

Conflict of Interest

The authors declare no conflict of interests.

References

Albalat R, Cañestro C. 2016. Evolution by gene loss. Nat. Rev. Genet. 17:379–391. doi: 10.1038/nrg.2016.39.

Andrews S. 2010. FastQC: A Quality Control Tool for High Throughput Sequence Data. https://www.bioinformatics.babraham.ac.uk/projects/fastqc/.

Arakane Y et al. 2005. The Tribolium chitin synthase genes TcCHS1 and TcCHS2 are specialized for synthesis of epidermal cuticle and midgut peritrophic matrix. Insect Mol. Biol. 14:453–463. doi: 10.1111/j.1365-2583.2005.00576.x.

Asano T, Seto Y, Hashimoto K, Kurushima H. 2019. Mini-review an insect-specific system for terrestrialization: Laccase-mediated cuticle formation. Insect Biochem. Mol. Biol. 108:61–70. doi: 10.1016/j.ibmb.2019.03.007.

Astashyn A et al. 2024. Rapid and sensitive detection of genome contamination at scale with FCS-GX. Genome Biol. 25:60. doi: 10.1186/s13059-024-03198-7.

Aurori CM et al. 2021. Juvenile hormone pathway in honey bee larvae: A source of possible signal molecules for the reproductive behavior of Varroa destructor. Ecol. Evol. 11:1057–1068. doi: 10.1002/ece3.7125.

Bairoch A. 2000. The ENZYME database in 2000. Nucleic Acids Res. 28:304–305. doi: 10.1093/nar/28.1.304.

Bello E, Chen Y, Alleyne M. 2022. Staying Dry and Clean: An Insect's Guide to Hydrophobicity. Insects. 14:42. doi: 10.3390/insects14010042.

Benoit JB, Denlinger DL. 2010. Meeting the challenges of on-host and off-host water balance in blood-feeding arthropods. J. Insect Physiol. 56:1366–1376. doi: 10.1016/j.jinsphys.2010.02.014.

Bernot JP et al. 2022. Chromosome-level genome assembly, annotation, and phylogenomics of the gooseneck barnacle Pollicipes pollicipes. GigaScience. 11:giac021. doi: 10.1093/gigascience/giac021.

Blaxter M et al. 2025. The Earth BioGenome Project Phase II: illuminating the eukaryotic tree of life. Front. Sci. 3:1514835. doi: 10.3389/fsci.2025.1514835.

Bonneton F, Laudet V. 2012. Evolution of nuclear receptors in insects. In: Insect Endocrinology. Elsevier pp. 219–252. doi: 10.1016/B978-0-12-384749-2.10006-8.

Burmester T. 2002. Origin and evolution of arthropod hemocyanins and related proteins. J. Comp. Physiol. [B]. 172:95–107. doi: 10.1007/s00360-001-0247-7.

Cabrera AR et al. 2015. Three Halloween genes from the Varroa mite, Varroa destructor (Anderson & Trueman) and their expression during reproduction. Insect Mol. Biol. 24:277–292. doi: 10.1111/imb.12155.

Camacho C et al. 2009. BLAST+: architecture and applications. BMC Bioinformatics. 10:421. doi: 10.1186/1471-2105-10-421.

Campbell MS et al. 2014. MAKER-P: A Tool Kit for the Rapid Creation, Management, and

Quality Control of Plant Genome Annotations. Plant Physiol. 164:513–524. doi: 10.1104/pp.113.230144.

Campli G et al. 2024. The moulting arthropod: a complete genetic toolkit review. Biol. Rev. Camb. Philos. Soc. doi: 10.1111/brv.13123.

Capella-Gutiérrez S, Silla-Martínez JM, Gabaldón T. 2009. trimAl: a tool for automated alignment trimming in large-scale phylogenetic analyses. Bioinformatics. 25:1972–1973. doi: 10.1093/bioinformatics/btp348.

Castellano KR et al. 2025. Genome Assembly of a Living Fossil, the Atlantic Horseshoe Crab *Limulus polyphemus* , Reveals Lineage-Specific Whole-Genome Duplications, Transposable Element-Based Centromeres, and a ZW Sex Chromosome System Wilson, M, editor. Mol. Biol. Evol. 42:msaf021. doi: 10.1093/molbev/msaf021.

Cheng H, Concepcion GT, Feng X, Zhang H, Li H. 2021. Haplotype-resolved de novo assembly using phased assembly graphs with hifiasm. Nat. Methods. 18:170–175. doi: 10.1038/s41592-020-01056-5.

Chipman AD. 2024. Arthropoda II: Mandibulata. In: Organismic Animal Biology. Oxford University PressOxford pp. 137–146. doi: 10.1093/oso/9780192893581.003.0023.

Chipman AD. 2025. The development and evolution of arthropod tagmata. Proc. R. Soc. B Biol. Sci. 292:20242950. doi: 10.1098/rspb.2024.2950.

Chipman AD et al. 2014. The First Myriapod Genome Sequence Reveals Conservative Arthropod Gene Content and Genome Organisation in the Centipede Strigamia maritima. PLOS Biol. 12:e1002005. doi: 10.1371/journal.pbio.1002005.

Daimon T, Uchibori M, Nakao H, Sezutsu H, Shinoda T. 2015. Knockout silkworms reveal a dispensable role for juvenile hormones in holometabolous life cycle. Proc. Natl. Acad. Sci. 112:E4226–E4235. doi: 10.1073/pnas.1506645112.

Denecke S et al. 2021. Comparative and functional genomics of the ABC transporter superfamily across arthropods. BMC Genomics. 22:553. doi: 10.1186/s12864-021-07861-2.

Didion JP, Martin M, Collins FS. 2017. Atropos: specific, sensitive, and speedy trimming of sequencing reads. PeerJ. 5:e3720. doi: 10.7717/peerj.3720.

Dixit R et al. 2008. Domain organization and phylogenetic analysis of proteins from the chitin deacetylase gene family of Tribolium castaneum and three other species of insects. Insect Biochem. Mol. Biol. 38:440–451. doi: 10.1016/j.ibmb.2007.12.002.

Dohmen E, Klasberg S, Bornberg-Bauer E, Perrey S, Kemena C. 2020. The modular nature of protein evolution: domain rearrangement rates across eukaryotic life. BMC Evol. Biol. 20:30. doi: 10.1186/s12862-020-1591-0.

Driscoll TP et al. 2020. A chromosome-level assembly of the cat flea genome uncovers rampant gene duplication and genome size plasticity. BMC Biol. 18:70. doi: 10.1186/s12915-020-00802-7.

Edgar RC. 2004. MUSCLE: multiple sequence alignment with high accuracy and high throughput. Nucleic Acids Res. 32:1792–1797. doi: 10.1093/nar/gkh340.

Fernández R, Gabaldón T. 2020. Gene gain and loss across the metazoan tree of life. Nat.

Ecol. Evol. 4:524–533. doi: 10.1038/s41559-019-1069-x.

Feron R, Waterhouse RM. 2022a. Assessing species coverage and assembly quality of rapidly accumulating sequenced genomes. GigaScience. 11:giac006. doi: 10.1093/gigascience/giac006.

Feron R, Waterhouse RM. 2022b. Exploring new genomic territories with emerging model insects. Curr. Opin. Insect Sci. 51:100902. doi: 10.1016/j.cois.2022.100902.

Feyereisen R. 2022. The P450 genes of the cat flea, *Ctenocephalides felis:* a CYPome in flux. Curr. Res. Insect Sci. 2:100032. doi: 10.1016/j.cris.2022.100032.

Fisk GJ, Thummel CS. 1995. Isolation, regulation, and DNA-binding properties of three Drosophila nuclear hormone receptor superfamily members. Proc. Natl. Acad. Sci. U. S. A. 92:10604–10608. https://www.ncbi.nlm.nih.gov/pmc/articles/PMC40660/ (Accessed September 12, 2024).

Flynn JM et al. 2020. RepeatModeler2 for automated genomic discovery of transposable element families. Proc. Natl. Acad. Sci. 117:9451–9457. doi: 10.1073/pnas.1921046117.

Flynn PC, Kaufman WR. 2015. Mechanical properties of the cuticle of the tick Amblyomma hebraeum (Acari: Ixodidae). J. Exp. Biol. 218:2806–2814. doi: 10.1242/jeb.123919.

Formenti G et al. 2022. Gfastats: conversion, evaluation and manipulation of genome sequences using assembly graphs Valencia, A, editor. Bioinformatics. 38:4214–4216. doi: 10.1093/bioinformatics/btac460.

Fukasawa Y, Ermini L, Wang H, Carty K, Cheung M-S. 2020. LongQC: A Quality Control Tool for Third Generation Sequencing Long Read Data. G3 GenesGenomesGenetics. 10:1193–1196. doi: 10.1534/g3.119.400864.

Fusco G, Minelli A. 2021. The Development of Arthropod Segmentation Across the Embryonic/Post-embryonic Divide – An Evolutionary Perspective. Front. Ecol. Evol. 9. doi: 10.3389/fevo.2021.622482.

Gabriel L et al. 2023. BRAKER3: Fully automated genome annotation using RNA-seq and protein evidence with GeneMark-ETP, AUGUSTUS and TSEBRA. doi: 10.1101/2023.06.10.544449.

Guan D et al. 2020. Identifying and removing haplotypic duplication in primary genome assemblies Valencia, A, editor. Bioinformatics. 36:2896–2898. doi: 10.1093/bioinformatics/btaa025.

Hensel R, Neinhuis C, Werner C. 2016. The springtail cuticle as a blueprint for omniphobic surfaces. Chem. Soc. Rev. 45:323–341. doi: 10.1039/C5CS00438A.

Hoang DT, Chernomor O, von Haeseler A, Minh BQ, Vinh LS. 2018. UFBoot2: Improving the Ultrafast Bootstrap Approximation. Mol. Biol. Evol. 35:518–522. doi: 10.1093/molbev/msx281.

Howard RJ, Puttick MN, Edgecombe GD, Lozano-Fernandez J. 2020. Arachnid monophyly: Morphological, palaeontological and molecular support for a single terrestrialization within Chelicerata. Arthropod Struct. Dev. 59:100997. doi: 10.1016/j.asd.2020.100997.

Hsiung B-K, Blackledge TA, Shawkey MD. 2015. Spiders do have melanin after all. J. Exp.

Biol. 218:3632–3635. doi: 10.1242/jeb.128801.

Huerta-Cepas J, Serra F, Bork P. 2016. ETE 3: Reconstruction, Analysis, and Visualization of Phylogenomic Data. Mol. Biol. Evol. 33:1635–1638. doi: 10.1093/molbev/msw046.

Janusz G et al. 2020. Laccase Properties, Physiological Functions, and Evolution. Int. J. Mol. Sci. 21:966. doi: 10.3390/ijms21030966.

Jindra M, Bellés X, Shinoda T. 2015. Molecular basis of juvenile hormone signaling. Curr. Opin. Insect Sci. 11:39–46. doi: 10.1016/j.cois.2015.08.004.

Jing X, Behmer ST. 2020. Insect sterol nutrition: Physiological mechanisms, ecology, and applications. Annu. Rev. Entomol. 65:251–271. doi: 10.1146/annurev-ento-011019-025017.

Jordan A et al. 2020. The potential of the solitary parasitoid *Microctonus brassicae* for the biological control of the adult cabbage stem flea beetle, *Psylliodes chrysocephala*. Entomol. Exp. Appl. 168:360–370. doi: 10.1111/eea.12910.

Kalyaanamoorthy S, Minh BQ, Wong TKF, von Haeseler A, Jermiin LS. 2017. ModelFinder: fast model selection for accurate phylogenetic estimates. Nat. Methods. 14:587–589. doi: 10.1038/nmeth.4285.

Katoh K, Standley DM. 2013. MAFFT Multiple Sequence Alignment Software Version 7: Improvements in Performance and Usability. Mol. Biol. Evol. 30:772–780. doi: 10.1093/molbev/mst010.

Kim Daehwan, Paggi JM, Park C, Bennett C, Salzberg SL. 2019. Graph-based genome alignment and genotyping with HISAT2 and HISAT-genotype. Nat. Biotechnol. 37:907–915. doi: 10.1038/s41587-019-0201-4.

Kim Jee-Hoon et al. 2019. Draft Genome Assembly of a Fouling Barnacle, Amphibalanus amphitrite (Darwin, 1854): The First Reference Genome for Thecostraca. Front. Ecol. Evol. 7. doi: 10.3389/fevo.2019.00465.

Kumar S et al. 2022. TimeTree 5: An Expanded Resource for Species Divergence Times. Mol. Biol. Evol. 39:msac174. doi: 10.1093/molbev/msac174.

Kuznetsov D et al. 2023. OrthoDB v11: annotation of orthologs in the widest sampling of organismal diversity. Nucleic Acids Res. 51:D445–D451. doi: 10.1093/nar/gkac998.

Langschied F et al. 2024. Quest for Orthologs in the Era of Biodiversity Genomics. Genome Biol. Evol. 16:evae224. doi: 10.1093/gbe/evae224.

Lees JG, Dawson NL, Sillitoe I, Orengo CA. 2016. Functional innovation from changes in protein domains and their combinations. Curr. Opin. Struct. Biol. 38:44–52. doi: 10.1016/j.sbi.2016.05.016.

Lerch S et al. 2020. Resilin matrix distribution, variability and function in Drosophila. BMC Biol. 18:195. doi: 10.1186/s12915-020-00902-4.

Lerch S, Yang Y, Flaven-Pouchon J, Gehring N, Moussian B. 2022. Resilin is needed for wing posture in Drosophila suzukii. Arch. Insect Biochem. Physiol. 111:e21913. doi: 10.1002/arch.21913.

Levy Karin E, Mirdita M, Söding J. 2020. MetaEuk—sensitive, high-throughput gene

discovery, and annotation for large-scale eukaryotic metagenomics. Microbiome. 8:48. doi: 10.1186/s40168-020-00808-x.

Li H et al. 2009. The Sequence Alignment/Map format and SAMtools. Bioinformatics. 25:2078–2079. doi: 10.1093/bioinformatics/btp352.

Li W, Godzik A. 2006. Cd-hit: a fast program for clustering and comparing large sets of protein or nucleotide sequences. Bioinformatics. 22:1658–1659. doi: 10.1093/bioinformatics/btl158.

Li Y, Zhang Z, Robinson GE, Palli SR. 2007. Identification and characterization of a juvenile hormone response element and its binding proteins. J. Biol. Chem. 282:37605–37617. doi: 10.1074/jbc.M704595200.

Manni M, Berkeley MR, Seppey M, Simão FA, Zdobnov EM. 2021. BUSCO Update: Novel and Streamlined Workflows along with Broader and Deeper Phylogenetic Coverage for Scoring of Eukaryotic, Prokaryotic, and Viral Genomes. Mol. Biol. Evol. 38:4647–4654. doi: 10.1093/molbev/msab199.

Mazzoni CJ, Ciofi C, Waterhouse RM. 2023. Biodiversity: an atlas of European reference genomes. Nature. 619:252–252. doi: 10.1038/d41586-023-02229-w.

McColgan Á, DiFrisco J. 2024. Understanding developmental system drift. Development. 151:dev203054. doi: 10.1242/dev.203054.

McNamara JC, Freire CA. 2022. Strategies of Invertebrate Osmoregulation: An Evolutionary Blueprint for Transmuting into Fresh Water from the Sea. Integr. Comp. Biol. 62:376–387. doi: 10.1093/icb/icac081.

Mendes FK, Vanderpool D, Fulton B, Hahn MW. 2021. CAFE 5 models variation in evolutionary rates among gene families. Bioinformatics. 36:5516–5518. doi: 10.1093/bioinformatics/btaa1022.

Michels J, Vogt J, Gorb SN. 2012. Tools for crushing diatoms – opal teeth in copepods feature a rubber-like bearing composed of resilin. Sci. Rep. 2:465. doi: 10.1038/srep00465.

Minh BQ et al. 2020. IQ-TREE 2: New Models and Efficient Methods for Phylogenetic Inference in the Genomic Era. Mol. Biol. Evol. 37:1530–1534. doi: 10.1093/molbev/msaa015.

Misof B et al. 2014. Phylogenomics resolves the timing and pattern of insect evolution. Science. 346:763–767. doi: 10.1126/science.1257570.

Mistry J, Bateman A, Finn RD. 2007. Predicting active site residue annotations in the Pfam database. BMC Bioinformatics. 8:298. doi: 10.1186/1471-2105-8-298.

Miyakawa H et al. 2013. A mutation in the receptor Methoprene-tolerant alters juvenile hormone response in insects and crustaceans. Nat. Commun. 4:1856. doi: 10.1038/ncomms2868.

Moussian B. 2010. Recent advances in understanding mechanisms of insect cuticle differentiation. Insect Biochem. Mol. Biol. 40:363–375. doi: 10.1016/j.ibmb.2010.03.003.

Moussian B. 2013. The Arthropod Cuticle. In: Arthropod Biology and Evolution. Minelli, A, Boxshall, G, & Fusco, G, editors. Springer Berlin Heidelberg: Berlin, Heidelberg pp. 171–

196. doi: 10.1007/978-3-642-36160-9_8.

Mrak P, Bogataj U, Štrus J, Žnidaršič N. 2017. Cuticle morphogenesis in crustacean embryonic and postembryonic stages. Arthropod Struct. Dev. 46:77–95. doi: 10.1016/j.asd.2016.11.001.

Nguyen L-T, Schmidt HA, von Haeseler A, Minh BQ. 2015. IQ-TREE: A Fast and Effective Stochastic Algorithm for Estimating Maximum-Likelihood Phylogenies. Mol. Biol. Evol. 32:268–274. doi: 10.1093/molbev/msu300.

Nijhout HF et al. 2014. The developmental control of size in insects. Wiley Interdiscip. Rev. Dev. Biol. 3:113–134. doi: 10.1002/wdev.124.

Niwa R et al. 2010. Non-molting glossy/shroud encodes a short-chain dehydrogenase/reductase that functions in the 'Black Box' of the ecdysteroid biosynthesis pathway. Development. 137:1991–1999. doi: 10.1242/dev.045641.

Nong W et al. 2021. Horseshoe crab genomes reveal the evolution of genes and microRNAs after three rounds of whole genome duplication. Commun. Biol. 4:83. doi: 10.1038/s42003-020-01637-2.

Okamoto N, Yamanaka N. 2021. Transporter-mediated ecdysteroid trafficking across cell membranes: A novel target for insect growth regulators. J. Pestic. Sci. 46:23–28. doi: 10.1584/jpestics.D20-071.

Okonechnikov K, Conesa A, García-Alcalde F. 2016. Qualimap 2: advanced multi-sample quality control for high-throughput sequencing data. Bioinformatics. 32:292–294. doi: 10.1093/bioinformatics/btv566.

de Oliveira AL, Calcino A, Wanninger A. 2019. Ancient origins of arthropod moulting pathway components VijayRaghavan, K & Martinez, P, editors. eLife. 8:e46113. doi: 10.7554/eLife.46113.

Osorio D, Rondón-Villarreal P, Torres R. 2015. Peptides: A Package for Data Mining of Antimicrobial Peptides. R J. 7:4–14. https://journal.r-project.org/archive/2015/RJ-2015-001/index.html (Accessed July 25, 2025).

Öztürk-Çolak A et al. 2024. FlyBase: updates to the Drosophila genes and genomes database. Genetics. 227:iyad211. doi: 10.1093/genetics/iyad211.

Pan X, Connacher RP, O'Connor MB. 2021. Control of the insect metamorphic transition by ecdysteroid production and secretion. Curr. Opin. Insect Sci. 43:11–20. doi: 10.1016/j.cois.2020.09.004.

Papadopoulou SmCh. 2006. *Tyrophagus putrescentiae* (Schrank) (Astigmata: Acaridae) as a new predator of *Lasioderma serricorne* (F.) (Coleoptera: Anobiidae) in tobacco stores in Greece. J. Stored Prod. Res. 42:391–394. doi: 10.1016/j.jspr.2005.06.004.

Paradis E, Schliep K. 2019. ape 5.0: an environment for modern phylogenetics and evolutionary analyses in R. Bioinforma. Oxf. Engl. 35:526–528. doi: 10.1093/bioinformatics/bty633.

Perrière G, Gouy M. 1996. WWW-query: an on-line retrieval system for biological sequence banks. Biochimie. 78:364–369. doi: 10.1016/0300-9084(96)84768-7.

Politi Y, Bertinetti L, Fratzl P, Barth FG. 2021. The spider cuticle: a remarkable material toolbox for functional diversity. Philos. Transact. A Math. Phys. Eng. Sci. 379:20200332. doi: 10.1098/rsta.2020.0332.

Qu Z et al. 2015. How Did Arthropod Sesquiterpenoids and Ecdysteroids Arise? Comparison of Hormonal Pathway Genes in Noninsect Arthropod Genomes. Genome Biol. Evol. 7:1951–1959. doi: 10.1093/gbe/evv120.

R Core Team. 2023. R: The R Project for Statistical Computing. https://www.r-project.org/ (Accessed October 29, 2024).

Ranallo-Benavidez TR, Jaron KS, Schatz MC. 2020. GenomeScope 2.0 and Smudgeplot for reference-free profiling of polyploid genomes. Nat. Commun. 11:1432. doi: 10.1038/s41467-020-14998-3.

Rehm P, Pick C, Borner J, Markl J, Burmester T. 2012. The diversity and evolution of chelicerate hemocyanins. BMC Evol. Biol. 12:19. doi: 10.1186/1471-2148-12-19.

Rewitz KF, Yamanaka N, Gilbert LI, O'Connor MB. 2009. The insect neuropeptide PTTH activates receptor tyrosine kinase torso to initiate metamorphosis. Science. 326:1403–1405. doi: 10.1126/science.1176450.

Reynolds SE. 1975. The mechanism of plasticization of the abdominal cuticle in Rhodnius. J. Exp. Biol. 62:81–98. doi: 10.1242/jeb.62.1.81.

Rhie A, Walenz BP, Koren S, Phillippy AM. 2020. Merqury: reference-free quality, completeness, and phasing assessment for genome assemblies. Genome Biol. 21:245. doi: 10.1186/s13059-020-02134-9.

Roer R, Abehsera S, Sagi A. 2015. Exoskeletons across the Pancrustacea: Comparative Morphology, Physiology, Biochemistry and Genetics. Integr. Comp. Biol. 55:771–791. doi: 10.1093/icb/icv080.

Samantsidis G-R et al. 2022. Functional characterization of putative ecdysone transporters in lepidopteran pests. Insect Biochem. Mol. Biol. 151:103830. doi: 10.1016/j.ibmb.2022.103830.

Sarmiento KP, Panes VA, Santos MD. 2016. Molecular cloning and expression of chitin deacetylase 1 gene from the gills of *Penaeus monodon* (black tiger shrimp). Fish Shellfish Immunol. 55:484–489. doi: 10.1016/j.fsi.2016.06.025.

Scherbaum S, Hellmann N, Fernández R, Pick C, Burmester T. 2018. Diversity, evolution, and function of myriapod hemocyanins. BMC Evol. Biol. 18:107. doi: 10.1186/s12862-018-1221-2.

Schumann I, Kenny N, Hui J, Hering L, Mayer G. 2018. Halloween genes in panarthropods and the evolution of the early moulting pathway in Ecdysozoa. R. Soc. Open Sci. 5:180888. doi: 10.1098/rsos.180888.

Schwentner M, Richter S, Rogers DC, Giribet G. 2018. Tetraconatan phylogeny with special focus on Malacostraca and Branchiopoda: highlighting the strength of taxon-specific matrices in phylogenomics. Proc. R. Soc. B Biol. Sci. 285:20181524. doi: 10.1098/rspb.2018.1524.

Sin YW et al. 2015. Identification of putative ecdysteroid and juvenile hormone pathway

genes in the shrimp Neocaridina denticulata. Gen. Comp. Endocrinol. 214:167–176. doi: 10.1016/j.ygcen.2014.07.018.

Smit AFA, Hubley R, Green P. 2013. RepeatMasker Open-4.0. http://www.repeatmasker.org.

Smykal V, Dolezel D. 2023. Evolution of proteins involved in the final steps of juvenile hormone synthesis. J. Insect Physiol. 145:104487. doi: 10.1016/j.jinsphys.2023.104487.

So WL et al. 2022. Myriapod genomes reveal ancestral horizontal gene transfer and hormonal gene loss in millipedes. Nat. Commun. 13:3010. doi: 10.1038/s41467-022-30690-0.

Stamatakis A. 2014. RAxML version 8: a tool for phylogenetic analysis and post-analysis of large phylogenies. Bioinformatics. 30:1312–1313. doi: 10.1093/bioinformatics/btu033.

Stolzer M et al. 2012. Inferring duplications, losses, transfers and incomplete lineage sorting with nonbinary species trees. Bioinformatics. 28:i409–i415. doi: 10.1093/bioinformatics/bts386.

van Straalen NM. 2021. Evolutionary terrestrialization scenarios for soil invertebrates. Pedobiologia. 87–88:150753. doi: 10.1016/j.pedobi.2021.150753.

Tegenfeldt F et al. 2025. OrthoDB and BUSCO update: annotation of orthologs with wider sampling of genomes. Nucleic Acids Res. 53:D516–D522. doi: 10.1093/nar/gkae987.

Tetlie OE, Brandt DS, Briggs DEG. 2008. Ecdysis in sea scorpions (Chelicerata: Eurypterida). Palaeogeogr. Palaeoclimatol. Palaeoecol. 265:182–194. doi: 10.1016/j.palaeo.2008.05.008.

Thomas GWC et al. 2020. Gene content evolution in the arthropods. Genome Biol. 21:15. doi: 10.1186/s13059-019-1925-7.

True JR, Haag ES. 2001. Developmental system drift and flexibility in evolutionary trajectories. Evol. Dev. 3:109–119. doi: 10.1046/j.1525-142x.2001.003002109.x.

Truman JW, Riddiford LM. 2022. Chinmo is the larval member of the molecular trinity that directs Drosophila metamorphosis. Proc. Natl. Acad. Sci. 119:e2201071119. doi: 10.1073/pnas.2201071119.

Ureña E, Chafino S, Manjón C, Franch-Marro X, Martín D. 2016. The occurrence of the holometabolous pupal stage requires the interaction between E93, Krüppel-Homolog 1 and Broad-Complex Desplan, C, editor. PLOS Genet. 12:e1006020. doi: 10.1371/journal.pgen.1006020.

Vargas HCM, Panfilio KA, Roelofs D, Rezende GL. 2021. Increase in egg resistance to desiccation in springtails correlates with blastodermal cuticle formation: Eco-evolutionary implications for insect terrestrialization. J. Exp. Zoolog. B Mol. Dev. Evol. 336:606–619. doi: 10.1002/jez.b.22979.

Wang X et al. 2022. FKBP39 Controls the Larval Stage JH Activity and Development in Drosophila melanogaster. Insects. 13:330. doi: 10.3390/insects13040330.

Waterhouse RM, Tegenfeldt F, Li J, Zdobnov EM, Kriventseva EV. 2013. OrthoDB: a hierarchical catalog of animal, fungal and bacterial orthologs. Nucleic Acids Res. 41:D358–

D365. doi: 10.1093/nar/gks1116.

Waterhouse RM, Zdobnov EM, Kriventseva EV. 2011. Correlating traits of gene retention, sequence divergence, duplicability and essentiality in vertebrates, arthropods, and fungi. Genome Biol. Evol. 3:75–86. doi: 10.1093/gbe/evq083.

Wellmeyer B, Böhringer AC, Rösner J, Merzendorfer H. 2023. Analyses of ecdysteroid transporters in the fat body of Tribolium castaneum. Insect Mol. Biol. 32:400–411. doi: 10.1111/imb.12839.

Wickham H. 2016. *ggplot2*. Springer International Publishing: Cham doi: 10.1007/978-3-319-24277-4.

Willis JH. 2010. Structural cuticular proteins from arthropods: annotation, nomenclature, and sequence characteristics in the genomics era. Insect Biochem. Mol. Biol. 40:189–204. doi: 10.1016/j.ibmb.2010.02.001.

Wong TKF et al. 2020. A minimum reporting standard for multiple sequence alignments. NAR Genomics Bioinforma. 2:lqaa024. doi: 10.1093/nargab/lqaa024.

Yoshiyama-Yanagawa T et al. 2011. The conserved Rieske oxygenase DAF-36/Neverland is a novel cholesterol-metabolizing enzyme. J. Biol. Chem. 286:25756–25762. doi: 10.1074/jbc.M111.244384.

Yuan J et al. 2024. An ancient whole-genome duplication in barnacles contributes to their diversification and intertidal sessile life adaptation. J. Adv. Res. 62:91–103. doi: 10.1016/j.jare.2023.09.015.

Zhang M et al. 2021. Roles of LmCDA1 and LmCDA2 in cuticle formation in the foregut and hindgut of Locusta migratoria. Insect Sci. 28:1314–1325. doi: 10.1111/1744-7917.12874.

Zhang Min et al. 2019. The putative chitin deacetylases Serpentine and Vermiform have non-redundant functions during Drosophila wing development. Insect Biochem. Mol. Biol. 110:128–135. doi: 10.1016/j.ibmb.2019.05.008.

Zhang Xiaojun et al. 2019. Penaeid shrimp genome provides insights into benthic adaptation and frequent molting. Nat. Commun. 10:356. doi: 10.1038/s41467-018-08197-4.

Zheng X et al. 2022. Transcriptome analysis reveals that SREBP modulates a large repertoire of genes involved in key cellular functions in Penaeus vannamei, although the majority of the dysregulated genes are unannotated. Genes. 13:2057. doi: 10.3390/genes13112057.

Figure Legends

Figure 1. Phylum-wide phylogeny reconstruction and orthology delineation.

(A) The order-level phylogeny shows the relationships and estimated divergence times of the 35 orders from the complete dataset of 145 arthropod species. The number of species in each order is shown in parentheses at each leaf of the tree. The phylogeny was estimated using a super-alignment of protein sequences from single-copy orthologues and time-calibrated with ten calibration nodes. The four major arthropod lineages are highlighted: Chelicerata (pink), Myriapoda (purple), Crustacea (yellow), and Hexapoda (green), where hexapods and the paraphyletic crustaceans together form the monophyletic Pancrustacea. **(B)** Orthology delineation at the level of the last common ancestor (LCA) of the complete dataset of 145 arthropod species resulted in the orthologous group (OG) dataset comprising a total of 74'214 OGs and 2'047'671 genes. Averaged across the species within each order, the bars show the counts of genes in OGs classified as single-copy (blue) or multi-copy (green, yellow) orthologues, or for which no orthologues could be identified (grey). **(C)** Assessing the phyletic ages of all OGs (left panel) shows just over a quarter can be traced to the arthropod LCA, while for the six functional modules of moulting machinery gene families (right panel) all but two gene families were traceable to the arthropod LCA. Phyletic ages were defined as the LCA of all the species included in each OG stratified to the levels of Arthropoda, Mandibulata (Pancrustacea + Myriapoda), the four subphyla, or younger than subphylum level. **(D)** The distributions of OG protein sequence divergence evolutionary rates for all OGs (left panel) and for the six functional modules of moulting machinery gene families (right panel). Moulting machinery families show overall significantly lower evolutionary rates than the background (Wilcoxon test, $p=1.258e-07$), and amongst the functional modules the ecdysteroid and sesquiterpenoid pathways are the most divergent (asterisks indicate Wilcoxon test p-values of *** $p<0.0005$; ** $p<0.005$, and * $p<0.05$). The boxplots show the median, first and third quartiles, and lower and upper extremes of the distribution (1.5 × Interquartile range).

Figure 2. Gene family copy-number profiling of the moulting machinery.

Phylogenetic profiling of gene copy numbers of families with evidence of involvement in various moulting processes quantified counts of identified orthologues across the 145-species dataset, partitioned by the 35 represented orders (rows) and six functional modules of the moulting machinery (columns). The four major arthropod lineages are coloured: Chelicerata (brick red), Myriapoda (lilac purple), Crustacea (peach orange), and Hexapoda (water green). Averaged proportions across the species within each order, the bars show the counts of genes in OGs classified as single-copy (blue) or multi-copy (green, yellow) orthologues, or for which no orthologues could be identified (deep purple). Gains and losses of genes involved in moulting are evident across all modules and nearly all orders: the sesquiterpenoid pathway and early genes modules exhibit mainly single-copy orthologues; the ecdysteroid pathway and late genes show elevated proportions of duplications/gains; and the neurostimuli reception module exhibits the lowest proportion of single-copy orthologues. This order by module profiling highlights broad trends, with the variability of the individual member gene families of each module detailed in Supplementary Figures 2-7. The cartoons above each functional module summarise the roles they play in moulting processes: the ecdysteroid pathway and sesquiterpenoid pathway for hormone synthesis and signalling, the early genes and fate genes for activation of the moult-inducing programme; the toolkit of receptors of neuropeptides switching on the moulting process, and downstream late gene effectors for exoskeleton renewal.

Figure 3. Moulting gene family copy-number profiling in myriapods.

Phylogenetic profiling of gene copy numbers of families involved in moulting across the three myriapod species sequenced and annotated in this study, namely the centipedes, *S. cingulata* and *S. coleoptrata*, and the millipede, *A. syriacus*. Orthologues are partitioned into six functional modules of the moulting machinery (named along the bottom of the figure). Cells show the counts of genes in orthologous groups (OGs) classified as single-copy (blue) or multi-copy (green, yellow) orthologues, or for which no orthologues could be identified (deep purple). Gains and losses of genes involved in moulting are evident across all modules and all three species: the ecdysteroid pathway and late genes show elevated proportions of duplications/gains, while in contrast the sesquiterpenoid pathway and early genes modules exhibit mainly single-copy orthologues. Full gene names are provided in Supplementary Figures 2-7.

Figure 4. Gene family and protein domain architecture dynamics of moulting gene families

(A) Ancestral state count reconstructions of gene family dynamics of moulting gene families. The state, or gene count, at internal nodes of the phylogeny is reconstructed from the observed gene copy numbers of the leaves (97 arthropod species), to infer changes in family sizes at each ancestral node. The phylogeny shows the four major arthropod lineages highlighted: Chelicerata (pink), Myriapoda (purple), Crustacea (yellow), and Hexapoda (green). To detect excess gene family expansions amongst moulting-related gene families compared to other gene families the number of families exhibiting gene gains at each node is compared between the moulting gene set and the background set using Fisher's exact test. Each node is annotated with a solid circle reporting the odds ratio (size) and strength of corrected p-values (colours, p.adj < 0.05 *, p.adj < 0.005 ** , p.adj < 0.0005 ***, NS not significant). Significant expansion excesses are evident at the LCA of each subphylum except Myriapoda, while no significant expansion excesses are found across the 35 ancestral nodes in the clade of eumetabolous insects (Holometabola and Paraneoptera). **(B)** Proportions of identified protein domain rearrangements explained with exact and non-ambiguous solutions for classification as fissions, fusions, single domain emergence or loss events, and terminal emergence or loss events. Rearrangement events in domain architectures were inferred by ancestral reconstructions comparing the moulting gene families set (foreground) and the background gene set of all families as old as the Arthropoda LCA (x-axis). Event type proportions are shown (y-axis) with each of the six event rearrangement types in the two sets coloured according to the legend. Background families reflect patterns previously found across multiple eukaryotic clades (Dohmen et al. 2020), in contrast, the arthropod moulting gene families exhibit a significantly reduced proportion of fusions (15.25%, odds ratio = 0.3, -log(p.adj) = 66), as well as elevated proportions of single domain emergences (1.31%, odds ratio = 4.6, -log(p.adj) = 7), terminal emergences (8.93%, odds ratio = 25, -log(p.adj) = 100) and terminal losses (34.42%, odds ratio = 1.6, -log(p.adj) = 12).

Figure 5. Confirming ancient gene duplications and lineage-wide losses.

Candidates identified from gene copy-number profiling as representing likely ancient duplications or lineage-wide losses were further investigated employing gene-tree species-tree reconciliation or gene searches of additional species with available genomes, respectively. **(A)** Reconciliations confirmed ancient and maintained gene duplications of key factors for exoskeleton remodelling at the LCAs of Mandibulata, Araneae, Chelicerata, and Pancrustacea. The duplication of the ancestral *CDA1/serp-CDA2/verm* chitin deacetylase gene occurred in the mandibulate ancestor, with an independent duplication also evident at the LCA of spiders, which additionally exhibits a maintained duplication of *Cda4*. The chitin synthases *kkv* and *Chs2* are characterised by two independent ancestral duplications, one in the chelicerate ancestor and the other in the ancestor of pancrustaceans. **(B)** Amongst the potential lineage-wide losses, genome searches recovered no PPO-like or hemocyanin-like genes in any other Arachnida lineages other than Araneae and Scorpiones (n=83 species), support for the putative emergence of *chinmo* in the copepod-hexapod ancestor implies subsequent losses in the other crustaceans (n=56) , E93 appears to have been lost from the class Branchiopoda (n=22) and most species of the order Sarcoptiformes (41/57), and *nvd* is confidently reported as missing from Coleoptera (n=251) and potentially from Mesostigmata (n=7).

Figure 6. Canonical cuticle protein content across Arthropoda

(A) Raw counts of proteins annotated as harbouring the canonical chitin-binding domain across arthropod subphyla (asterisks indicate phylANOVA test p-values of *p<0.05). **(B)** Cuticle Protein (CP) repertoire redundancy. CPs are clustered within-species by 80% sequence similarity, and the ratio of clusters to counts approximates repertoire redundancy, with lower values indicating more sets of CPs with high sequence similarity (asterisks indicate phylANOVA test p-values of *p<0.05) **(C)** CP physico-chemical properties. Each data point represents the average value of all CPs found in a species for the isoelectric point, the aliphatic index, and the hydrophobic moment index (asterisks indicate phylANOVA test p-values of ** p<0.005, and *p<0.05).

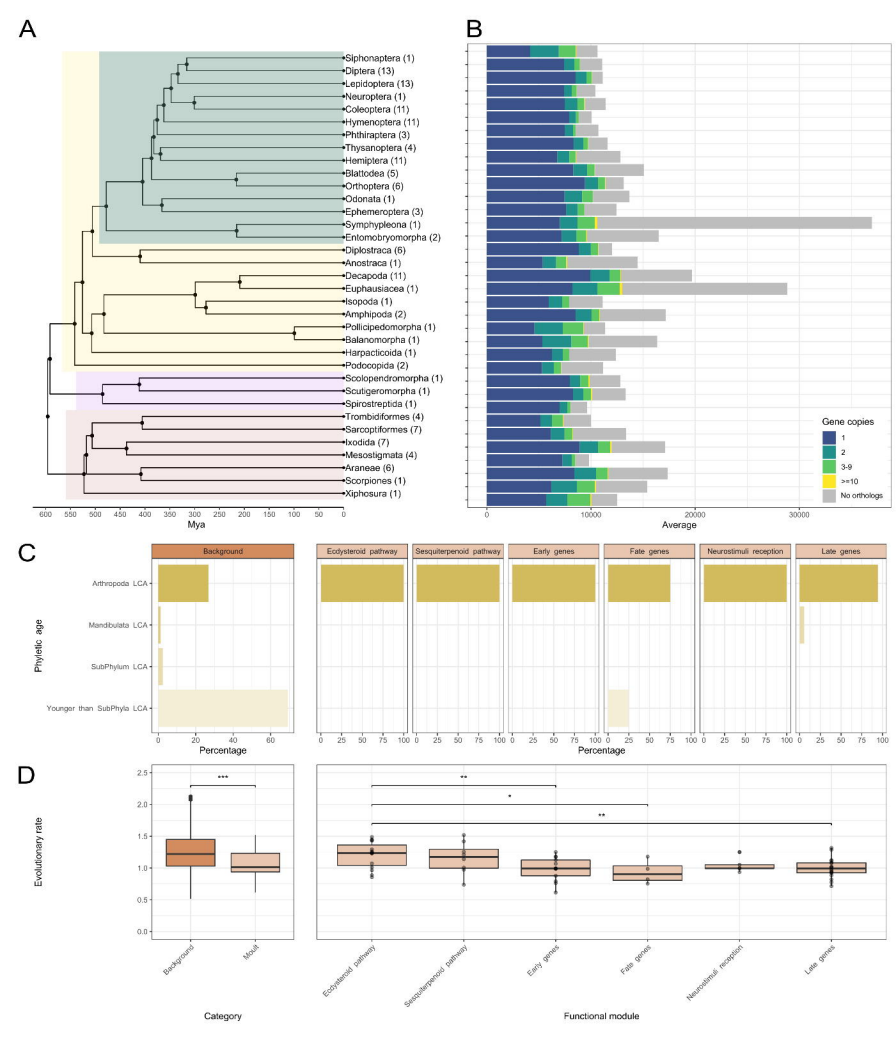
A
Siphonaptera (1)
Diptera (13)
Lepidoptera (13)
Neuroptera (1)
Coleoptera (11)
Hymenoptera (11)
Phthiraptera (3)
Thysanoptera (4)
Hemiptera (11)
Blattodea (5)
Orthoptera (6)
Odonata (1)
Ephemeroptera (3)
Symphypleona (1)
Entomobryomorpha (2)
Diplostraca (6)
Anostraca (1)
Decapoda (11)
Euphausiacea (1)
Isopoda (1)
Amphipoda (2)
Pollicipedomorpha (1)
Balanomorpha (1)
Harpacticoida (1)
Podocopida (2)
Scolopendromorpha (1)
Scutigeromorpha (1)
Spirostreptida (1)
Trombidiformes (4)
Sarcoptiformes (7)
Ixodida (7)
Mesostigmata (4)
Araneae (6)
Scorpiones (1)
Xiphosura (1)
600 550 500 450 400 350 300 250 200 150 100 50 0
Mya
B
Gene copies
1
2
3-9
>=10
No orthologs
0 10000 20000 30000
Average
C
Background
Ecdysteroid pathway
Sesquiterpenoid pathway
Early genes
Fate genes
Neurostimuli reception
Late genes
Phyletic age
Arthropoda LCA
Mandibulata LCA
SubPhylum LCA
Younger than SubPhyla LCA
0 20 40 60
Percentage
0 25 50 75 100
Percentage
D
Evolutionary rate
0.0 0.5 1.0 1.5 2.0 2.5
***
**
*
**
Background
Module
Category
Ecdysteroid pathway
Sesquiterpenoid pathway
Early genes
Fate genes
Neurostimuli reception
Late genes
Functional module

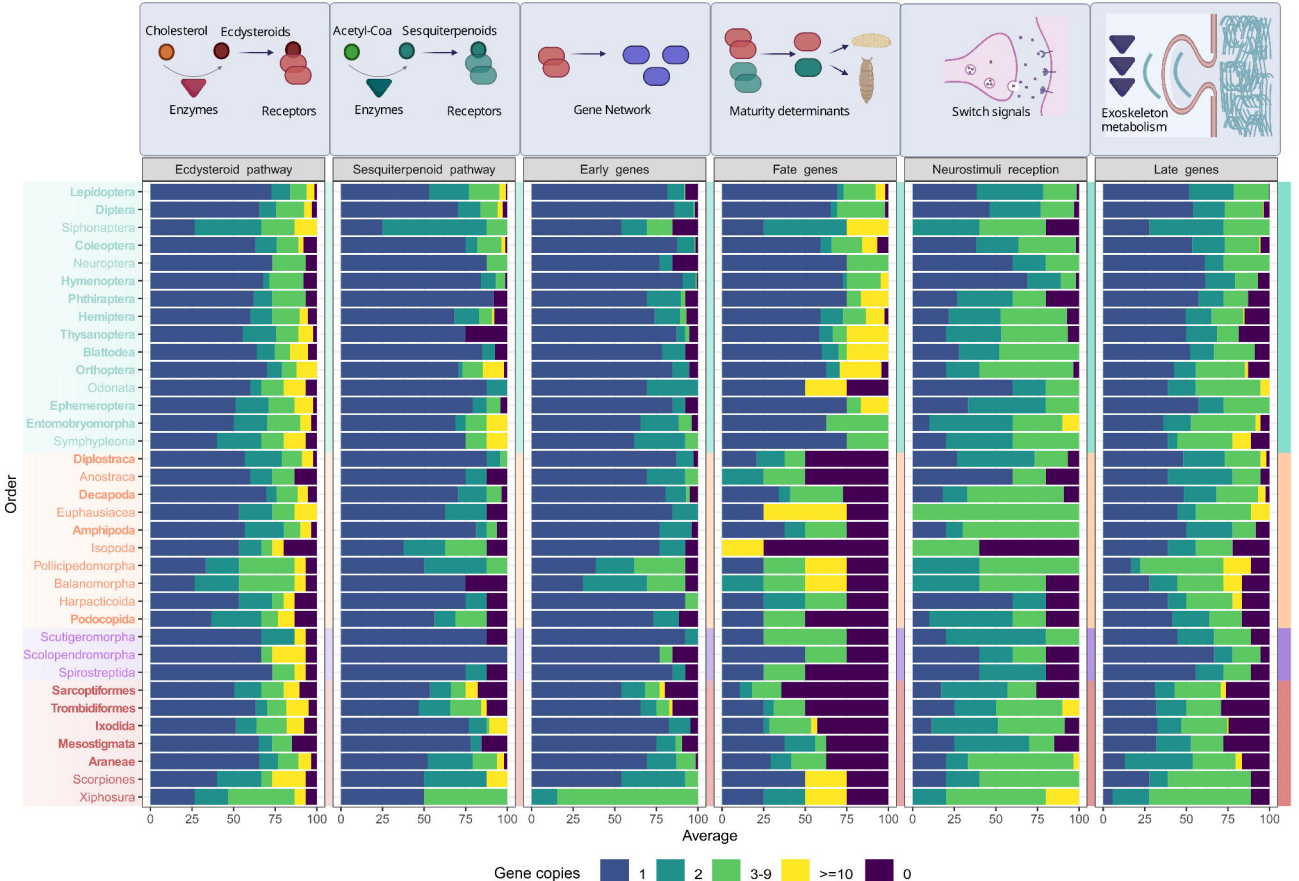
Cholesterol
Ecdysteroids
Enzymes
Receptors
Acetyl-Coa
Sesquiterpenoids
Enzymes
Receptors
Gene Network
Maturity determinants
Switch signals
Exoskeleton metabolism
Ecdysteroid pathway
Sesquiterpenoid pathway
Early genes
Fate genes
Neurostimuli reception
Late genes
Order
Lepidoptera
Diptera
Siphonaptera
Coleoptera
Neuroptera
Hymenoptera
Phthiraptera
Hemiptera
Thysanoptera
Blattodea
Orthoptera
Odonata
Ephemeroptera
Entomobryomorpha
Symphypleona
Diplostraca
Anostraca
Decapoda
Euphausiacea
Amphipoda
Isopoda
Pollicipedomorpha
Balanomorpha
Harpacticoida
Podocopida
Scutigeromorpha
Scolopendromorpha
Spirostreptida
Sarcoptiformes
Trombidiformes
Ixodida
Mesostigmata
Araneae
Scorpiones
Xiphosura
0
25
50
75
100
Average
Gene copies
1
2
3-9
>=10
0

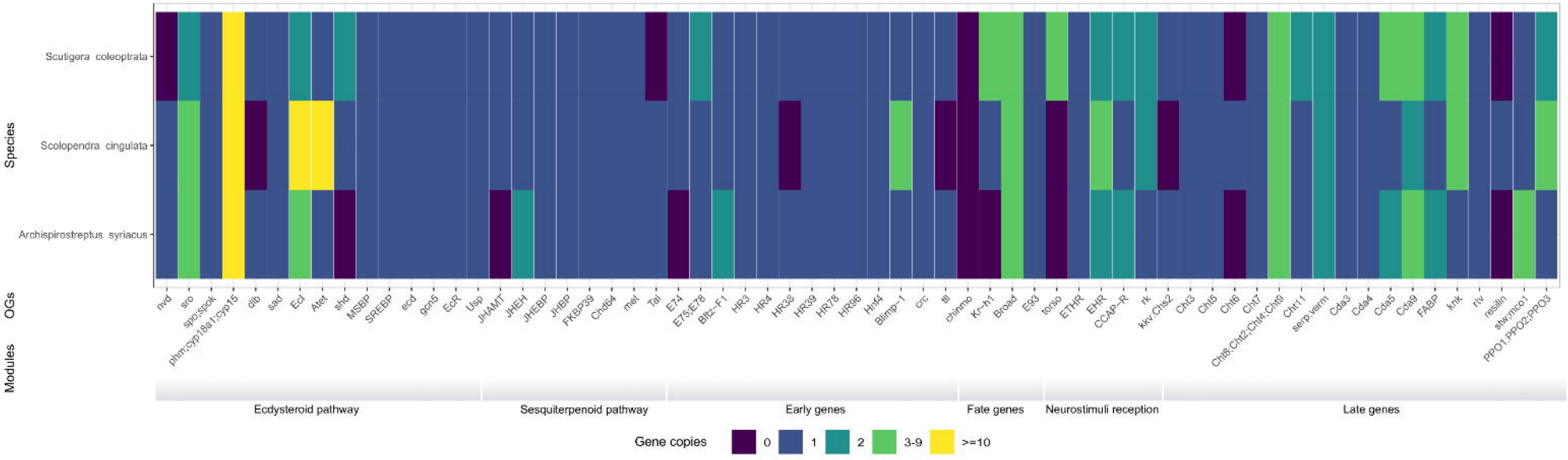
Species
Scutigera coleoptrata
Scolopendra cingulata
Archispirostreptus syriacus
OGs
nvd
sro
spo;spok
phm;cyp18a1;cyp15
dib
sad
Ecl
Atet
shd
MSBP
SREBP
ecd
gon5
EcR
Usp
JHAMT
JHEH
JHEBP
JHBP
FKBP39
Chd64
met
Tai
E74
E75;E78
Bftz-F1
HR3
HR4
HR38
HR39
HR78
HR96
Hnf4
Blimp-1
crc
tll
chinmo
Kr-h1
Broad
E93
torso
ETHR
EHR
CCAP-R
rk
kkv;Chs2
Chi3
Chi5
Chi6
Chi7
Cht8;Cht2;Cht4;Cht9
Cht11
serp;verm
Cda3
Cda4
Cda5
Cda9
FABP
knk
rtv
resilin
stwi;mco1
PPO1;PPO2;PPO3
Modules
Ecdysteroid pathway
Sesquiterpenoid pathway
Early genes
Fate genes
Neurostimuli reception
Late genes
Gene copies
0
1
2
3-9
>=10

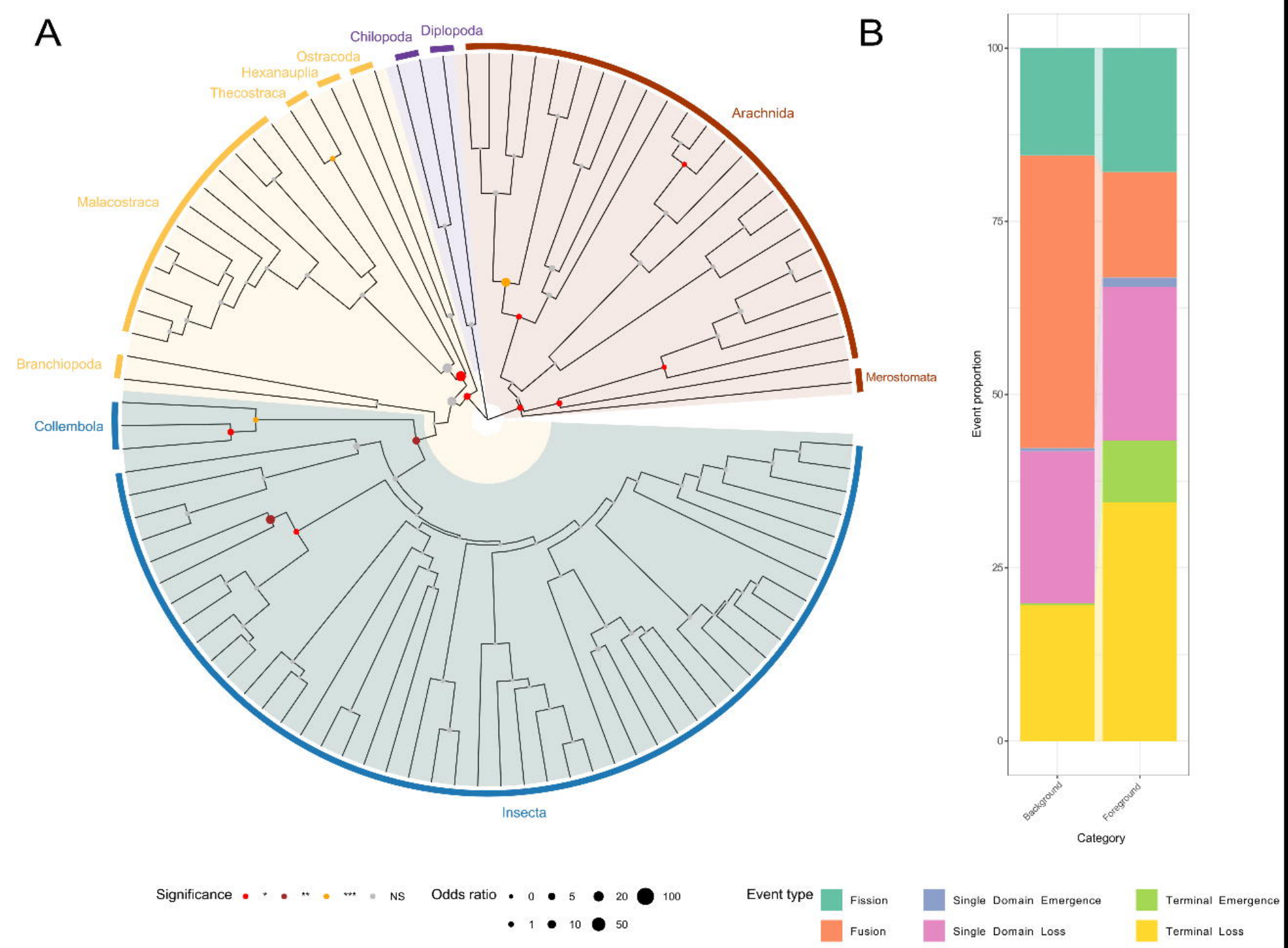
A
Chilopoda
Diplopoda
Ostracoda
Hexanauplia
Thecostraca
Arachnida
Malacostraca
Branchiopoda
Merostomata
Collembola
Insecta
B
Event proportion
100
75
50
25
0
Background
Foreground
Category
Significance
*
**
***
NS
Odds ratio
0
5
20
100
1
10
50
Event type
Fission
Fusion
Single Domain Emergence
Single Domain Loss
Terminal Emergence
Terminal Loss

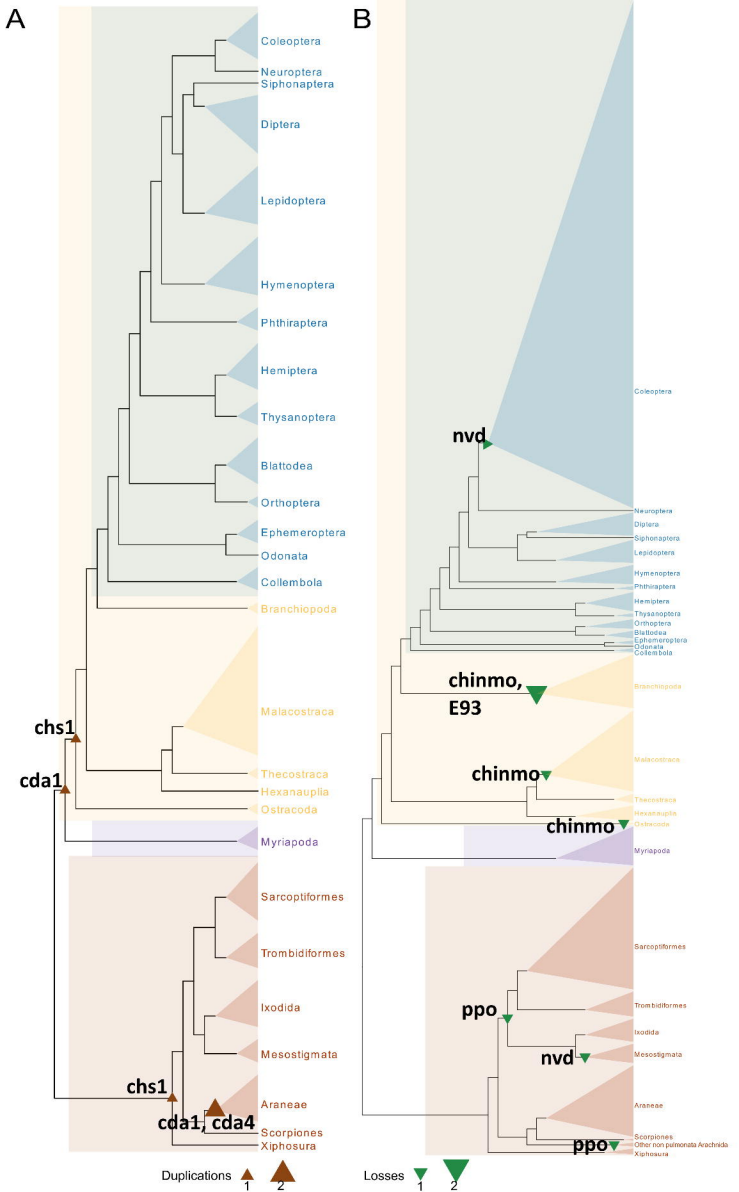
A
Coleoptera
Neuroptera
Siphonaptera
Diptera
Lepidoptera
Hymenoptera
Phthiraptera
Hemiptera
Thysanoptera
Blattodea
Orthoptera
Ephemeroptera
Odonata
Collembola
Branchiopoda
Malacostraca
Thecostraca
Hexanauplia
Ostracoda
Myriapoda
Sarcoptiformes
Trombidiformes
Ixodida
Mesostigmata
Araneae
Scorpiones
Xiphosura
chs1
cda1
chs1
cda1, cda4
Duplications
1
2
B
nvd
chinmo,
E93
chinmo
chinmo
ppo
nvd
ppo
Losses
1
2

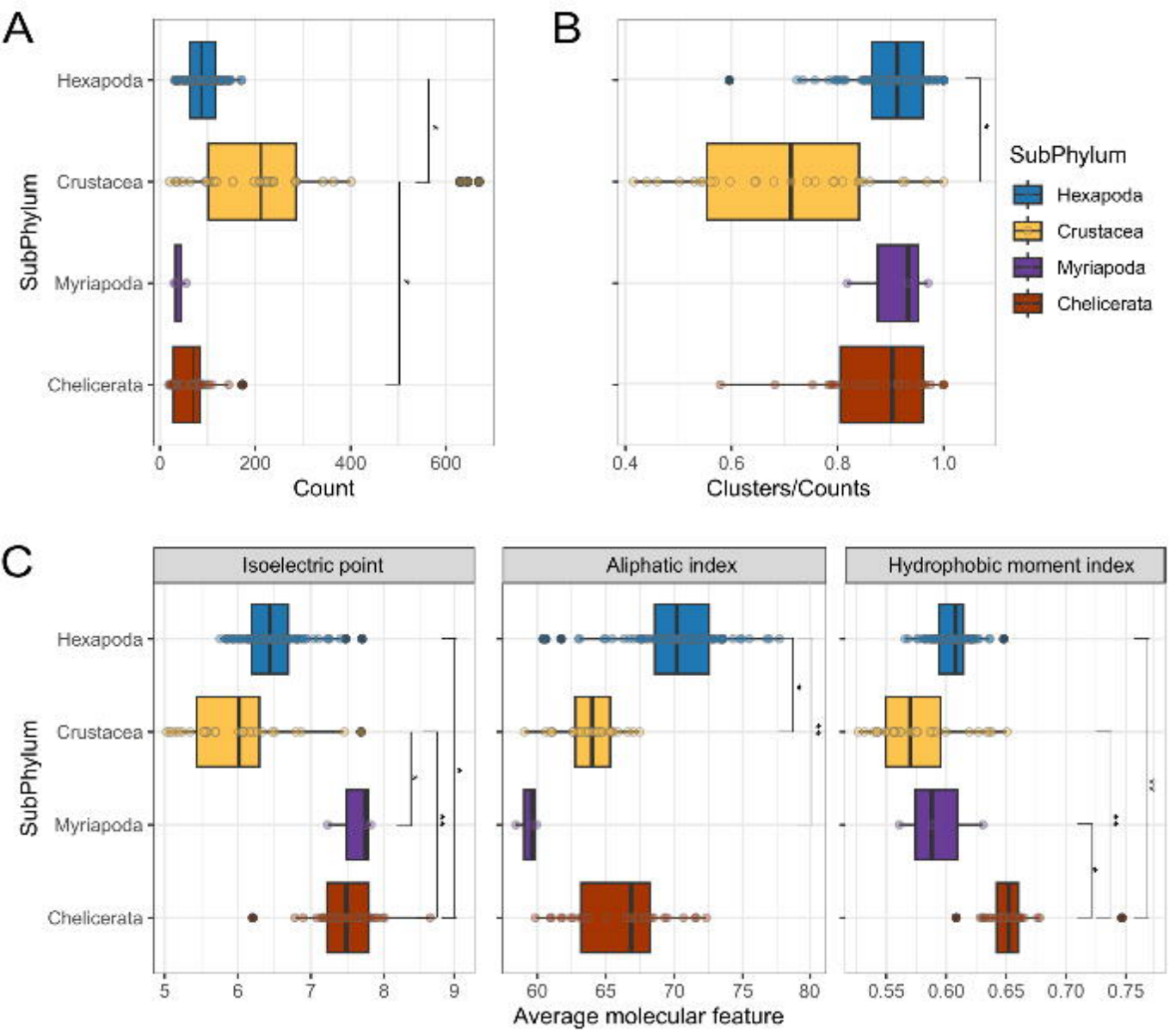
A
B
C
SubPhylum
Hexapoda
Crustacea
Myriapoda
Chelicerata
Count
Clusters/Counts
Isoelectric point
Aliphatic index
Hydrophobic moment index
Average molecular feature